J. Fluid Mech. (1992), *vol.* 234, *pp.* 361–391
Printed in Great Britain

The jet edge-tone feedback cycle; linear theory for the operating stages

By D. G. CRIGHTON
Department of Applied Mathematics and Theoretical Physics, University of Cambridge, Silver Street, Cambridge CB3 9EW, UK

(Received 11 June 1987 and in revised form 7 June 1991)

The paper presents a linear analytical model to predict the frequency characteristics of the discrete oscillations of the jet-edge feedback cycle. The jet is idealized as having top-hat profile with vortex-sheet shear layers, and the nozzle from which it issues is represented by a parallel plate duct. At a stand-off distance h, a flat plate is inserted along the centreline of the jet, and a sinuous instability wave with real frequency ω is assumed to be created in the vicinity of the nozzle and to propagate towards the splitter plate. Its interaction with the splitter plate produces an irrotational feedback field which, near the nozzle exit, is a periodic transverse flow producing singularities at the nozzle lips. Vortex shedding is assumed to occur, alleviating the singularities and allowing a trailing-edge Kutta condition to be satisfied; this Kutta condition is claimed to be the phase-locking criterion. The shed vorticity develops into a sinuous spatial instability, and the cycle of events is repeated periodically.

Problems corresponding to the various physical processes described are analysed, for inviscid flow with vortex-sheet shear layers and aligned flat-plate boundaries, and solved in an appropriate asymptotic sense by Wiener–Hopf methods. Calculation of the phase changes occurring in the constituents of the cycle gives an equation for the frequency ω in the Nth 'stage' as a function of jet width $2b$, jet velocity U_0, stand-off distance h, and stage label N:

$$\omega b/U_0 = (b/h)^{\frac{3}{2}}[4\pi(N-\tfrac{3}{8})]^{\frac{3}{2}}.$$

The variations with b, U_0, h and N are in excellent agreement with edge-tone experiments; the principal disagreement lies in the overall numerical factor $(4\pi)^{\frac{3}{2}}$ and explanations are given for this. Possible effects associated with the inclusion of displacement thickness fluctuations in the splitter-plate boundary layers, and the enforcement of a leading-edge Kutta condition, are also considered and shown not to affect the frequencies of the operating stages.

Contents

1. Introduction

Scientific study of the generation of discrete frequency hydrodynamic fluctuations and associated acoustic tones in shear-layer flows coupled to solid boundaries with sharp edges has now gone on for well over a century. Flows of this kind are essential components of many engineering devices, and of several wind instruments, and are often inadvertently introduced into other configurations and devices. Discrete tones are frequently associated with undesirable effects, such as very high near-field pressures inducing structural fatigue, or intense far-field pressures with considerable annoyance value. Understanding of these flows is therefore an important problem, whose solution may lead to avoidance or mitigation of high near- or far-field pressures in engineering applications, and to the design of improved musical instruments.

Theoretical study of elements of these flows has also gone on for more than a century, since the first studies by Helmholtz and Rayleigh of the instability of vortex sheets and plane jets. The full problem is one of great complexity, involving the interaction between vortical and acoustic modes at large bounding surfaces with sharp leading and trailing edges, the vortical modes themselves being spatial instabilities of a non-uniform flow which suffer strong amplification and nonlinear roll-up into concentrations of vorticity. Progress has, accordingly, involved a considerable amount of empirical input, and all models so far proposed can be criticized for the gaps which they leave between those individual elements of discrete tone flows which do permit rational analytical study.

This paper offers a start on a systematic and rational analysis of all the processes occurring in perhaps the best-known such flow – the so-called *jet edge-tone*. Here, discrete tones, in the flow itself and in the acoustic field, are produced when a wedge is placed in an essentially two-dimensional jet issuing from a nozzle of high aspect ratio. The idealized model to be studied here is sketched in figure 1, where the wedge is contracted down to a semi-infinite flat plate aligned with the flow. Actual experiments have used a wide range of wedge angles, and indeed qualitatively similar effects are produced when a bluff cylinder is placed across the flow, so that this particular aspect of the model in figure 1 ought to be adequate to reveal the main features. Actual experiments also involve a very wide range of upstream geometries; many different aspect ratios have been used, while in some experiments the jet issues from a slit in a large plane wall, in others a nozzle, sometimes with a long parallel section, sometimes with only a rapid contraction section, is used. We have taken the jet to be formed by two semi-infinite parallel plates, because this is the only configuration for which an exact calculation can be made of the interaction of an unsteady crossflow with the jet and nozzle, and of the continuous shedding of vorticity from the nozzle edge. This modelling is unexceptionable, and as representative of a typical nozzle as any other.

The jet itself is taken as a top-hat jet with uniform flow between two vortex-sheet shear layers. This permits analytical investigation of the jet coupling to the nozzle and the jet interaction with the downstream splitter plate, processes which cannot be easily analysed with a more 'realistic' profile (although Goldstein 1981 has

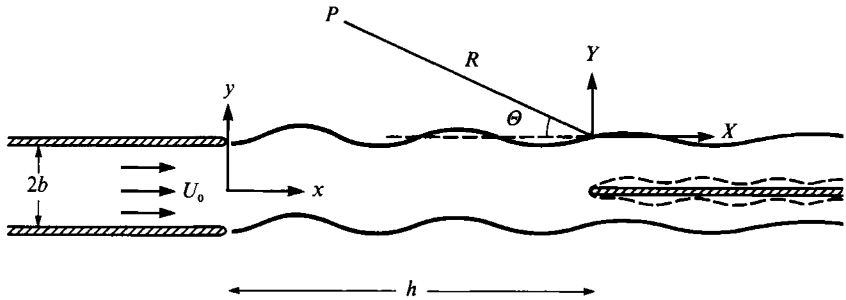

FIGURE 1. Schematic of the edge-tone model configuration studied in the paper: , vortex-sheet boundaries of the jet; , displacement thickness fluctuations on the splitter-plate boundary layers; , rigid walls aligned with the mean flow; duct walls and splitter plate. The jet has width $2b$, uniform velocity U_0, and the stand-off distance is h. With respect to the $0XY$ frame, polar coordinates are given by $X = -R\cos\Theta$, $Y = R\sin\Theta$.

extracted considerable detail for more general smooth profiles for the splitter-plate problem, while leaving open the question of how to deal with the nozzle interaction). Most experiments have not involved anything like a top-hat profile, and indeed many investigators have gone to some pains to assure themselves that their jet emerged from the nozzle with a fully developed parabolic profile. That seems, however, to be an inessential precaution, and recent studies of both low- and high-speed jets with uniform top-hat profiles (at exit, at least) by Krothapalli & Horne (1984) have shown all the features seen with parabolic profiles. In fact they have shown more, in the sense that while it is generally believed (on the basis of parabolic profile experiments) that the edge-tone system oscillates with at most one discrete frequency for specified values of the geometrical and flow parameters, the results for top-hat profiles clearly show the coexistence of several discrete tones, even in the low-speed case.

Certain general features are common to most discrete-tone flows. For extensive discussions of these and for much further background, the reader is referred to the reviews by Rockwell & Naudascher (1979) and Blake & Powell (1986), while the edge-tone itself is the focus of the review by Karamcheti *et al.* (1969). The role of the edge-tone type of configuration and mechanism in the sounding of wind instruments is discussed in the review by Fletcher (1979). In terms specifically of the edge-tone, and of features associated with the hydrodynamics rather than the acoustics, the observations may be summarized as follows:

(i) oscillations of the jet system take place in a set of stages, Stage I, II, etc., in each of which the (radian) frequency ω varies with duct width $2b$, exit flow velocity U_0 and stand-off distance h in a definite way which is only very weakly dependent on Reynolds number;

(ii) in a given stage, ω increases linearly with U_0, and decreases with h as some power between -1 and $-\frac{3}{2}$;

(iii) there is a minimum speed, for given h, below which no tones are generated, and a minimum stand-off distance for given U_0;

(iv) in some cases there is hysteresis, the stages overlapping and the jump from one stage to another occurring at different values (of h, say) depending on whether h is increasing or decreasing, while in others there is no hysteresis, while in yet others several tones of comparable amplitude are present simultaneously.

Features of the acoustic field – such as its directivity – are neither so clear nor so widely accepted, and will not be discussed in the present paper.

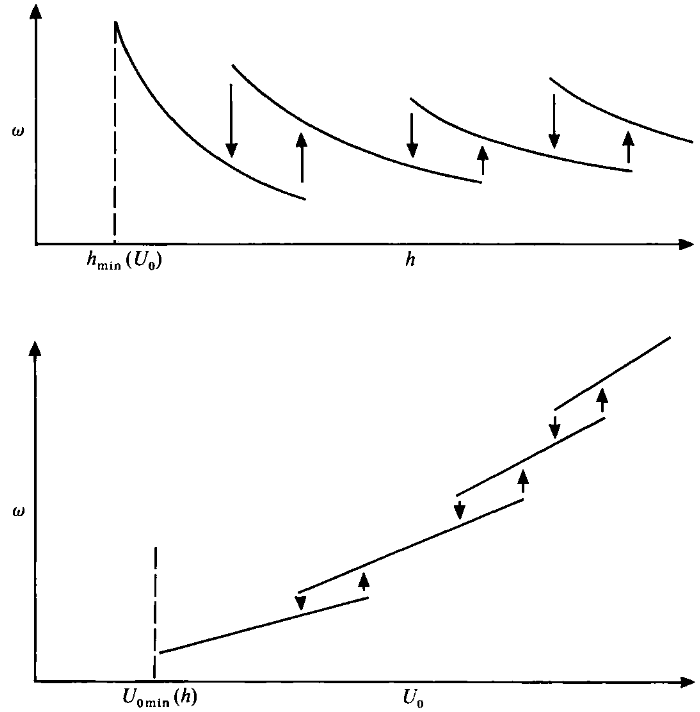

FIGURE 2. Schematic of the variation, in a typical experiment, of the observed frequency ω of discrete tone oscillation with stand-off distance h (U_0, b fixed) and with velocity U_0 (h, b fixed). In the diagram, though not always in an experiment, a single tone is present at any condition provided $U_0 > U_{0\,min}(h)$ and $h > h_{min}(U_0)$; and there is hysteretic jumping between the stages of oscillation.

Our aim is to provide a linear theory to account for features (i) and (ii) (illustrated schematically in figure 2) – and in particular to provide a clear-cut criterion for the phase-locking which determines the existence of possible stages of periodic oscillation. The theory amounts to a quantification of an idea first made explicit by Powell (1961), and only in part quantified by others. The idea is that any discrete-tone flow constitutes a 'feedback cycle'. A disturbance originating at the nozzle exit frees itself from the influence of the nozzle and then propagates freely – as a developing wave-like instability on the jet – eventually rolling up into a 'street' of coherent vortices, until it interacts with the splitter plate or wedge. Here it generates an irrotational field which is 'fed back' (instantaneously, in incompressible flow) to the vicinity of the nozzle where it forces the release of a later disturbance at precisely the right phase to sustain the cycle. The semi-infinite plate and the wedge have qualitatively identical properties as far as the feedback field is concerned. They each cause a 'mode conversion' at the edge, an incident sinuous mode (with boundary condition $\phi = 0$ on the jet centreline) being converted into a varicose mode (with hard-wall boundary condition $\partial\phi/\partial n = 0$) on each of the two streams into which the jet divides. The discrete mode conversion is smoothed out by the generation of an irrotational field, and it is this that is the feedback field, significant at large distances upstream.

If one could trace the (complex) efficiencies or *effectivenesses* η_j (Powell 1961) with which these processes are carried out in the complete feedback loop, their product would have to come to unity,

$$A = \prod \eta_j = 1, \tag{1.1}$$

or $|A| = 1, \arg A = 2N\pi$, so that the amplitude gain is zero (decibels), while the phase change is an integer multiple of 2π. We shall derive a 'dispersion relation' of precisely the form (1.1), from which we shall claim the frequency stages to be given by the (real) roots for ω of the phase content of (1.1),

$$\arg A = 2N\pi. \tag{1.2}$$

Such real ω do not allow the amplitude condition simultaneously to be satisfied, nor should we expect this to be possible. We assert – and will try to demonstrate, in extensions of this study to include several nonlinear effects – that a nonlinear theory would allow the complete (1.1) to be satisfied with real ω close to those obtained from the linear phase relation (1.2); nonlinear effects have a large influence on the amplitudes (in particular on the spatial amplification of instability waves in the jet) but a much smaller influence on both the local transverse structure of those instabilities and on their dispersion characteristics (in particular the variation of wavelength with frequency and the jet velocity and width). A great deal of evidence has now been accumulated from studies of large-scale coherent structures in turbulent shear flows to substantiate this claim; see, for example, Strange & Crighton (1983), Gaster, Kit & Wygnanski (1985), Cohen & Wygnanski (1987*a*, *b*), where linear theory is shown to work extremely well except with regard to instability growth (for which standard linear theory is also shown to be greatly improved by incorporation of linear mean-flow divergence effects). In particular, linear theory is shown in these papers to provide a very accurate prediction of transverse mode shape and phase characteristics, even for quite strongly nonlinear disturbances, though the mode shapes and phases are sensitive to detail of the mean velocity profile.

An alternative attitude towards our approach is the following. We wish to calculate frequencies from a phase-locking condition

$$\sum_j \arg \eta_j = 2N\pi, \tag{1.3}$$

and we argue on the basis of the experimental evidence that the phase changes $\arg \eta_j$ can be calculated approximately from linear theory. It is simply *convenient* to calculate the complete relation (1.1) from linear theory, and then to select the desired phase content (1.3).

A linear theory would not be expected to answer questions of hysteretic behaviour – on which in any case there are conflicting claims in the literature, nor could it give the amplitude of the sound field. It might, however, be expected to give the directivity of the sound field, and some scaling laws, but that is not an issue we take up in this paper, because the matching of the incompressible field determined in this paper to an outer acoustic field turns out to be surprisingly complicated. Accordingly, we defer consideration of nonlinear hydrodynamic effects, and of the acoustic field in linear theory, to later papers, and concentrate here on the possible stages of periodic motion. A crucial point in the analysis is the phase-locking condition, and we propose here that this condition involves satisfaction of a Kutta condition at the (trailing) edges of the nozzle. Crighton (1985) gives a review of the status of the Kutta condition in a range of unsteady flows, and at leading and trailing edges and points of separation on smooth bodies. It can be confidently assumed that the condition holds at the trailing edges (in the sense that all velocities predicted by inviscid theory must be finite at those edges) in the ranges of frequency, fluctuation amplitude and Reynolds number appropriate to normal laboratory edge-tone operation. A vorticity-shedding criterion has actually recently been used in acoustic feedback resonance problems studied numerically by Hourigan *et al.* (1990) and Stoneman *et al.* (1988). The authors state explicitly that 'the shedding...does not involve the Kutta condition', as the bodies concerned are smooth, but there is nevertheless a shedding at a definite rate which would correspond mathematically to that dictated by a Kutta condition if the zero-thickness-sharp-edge limit were taken.

Applicability of a Kutta condition at the leading edge of the splitter plate is not, however, on such a firm footing, and for most of the paper we accept the usual inverse-square-root velocity singularity there. Section 9 then attempts to model displacement thickness fluctuations in the boundary layers over the splitter plate (Howe 1981 *a*, *b*, *c*) and to determine their amplitude so as to impose the leading-edge Kutta condition. It is found that this imposition makes no difference at all to the function in (1.2), and hence the stage frequencies remain unchanged, but the acoustic field is significantly changed, in a way to be described in a future paper on the acoustics of the edge-tone.

Our approach differs from that of previous workers in the following respects:

(i) it consistently calculates all phase changes from the exact solution of linear problems from the same model without *ad hoc* assumptions or approximations;

(ii) it claims the Kutta condition as the phase-locking criterion.

Other workers have calculated contributions to the net phase change from various different models. Karamcheti *et al.* (1969) calculated the phase changes for the amplifying instability wave on the jet, using a parabolic form for the velocity profile and including the effects of slow divergence of the mean profile with downstream distance. Interaction of such a jet with either the nozzle walls or the splitter plate is not easily handled, however, nor was it. Curle (1953) and Holger, Wilson & Beavers (1977) represented the jet instead by an array of concentrated vortices, which allows detailed treatment, by conformal mapping, of the passage of the vortices past a wedge (of non-zero angle, if required) downstream. But such a representation does not correctly model the behaviour near the jet exit, where the vortices are far from fully formed (see figure 3), and where correct modelling of the flow is essential for application of the Kutta condition; and it does not take into account the unstable growth of perturbations in the jet which is essential to offset the algebraically decaying feedback field from the downstream body.

While acknowledging the importance of each of the contributions mentioned to improved understanding of particular elements of the cycle, we believe that the model sketched in figure 1 and analysed in this paper is the first to put all the necessary features together consistently.

The organization of this paper is as follows. An exact formulation is given in §2 of the boundary-value problem corresponding to figure 1, and it is argued that it is appropriate to seek a solution under the asymptotic limit $b \ll \lambda_0 \ll h$, where λ_0 is the wavelength of the jet instability. This permits the problem to be decoupled into a series of analytically tractable problems, and corresponds to the physical picture which is always in mind when one describes the edge-tone (and other flows) in feedback cycle terms. It means that the jet is not closely coupled simultaneously to upstream and downstream boundaries, but rather that essentially different physical processes occur in different regions of space. We consider in §3 how a freely amplifying spatial instability mode of the sinuous kind interacts with the splitter plate – the exponential amplification implying that the nozzle can be regarded as at 'minus infinity'. As part of the downstream interaction, we calculate (§4) the irrotational algebraically decaying field which, near the nozzle, looks like a transverse oscillatory streaming, and in §5 how the jet responds to this cross-stream forcing. In

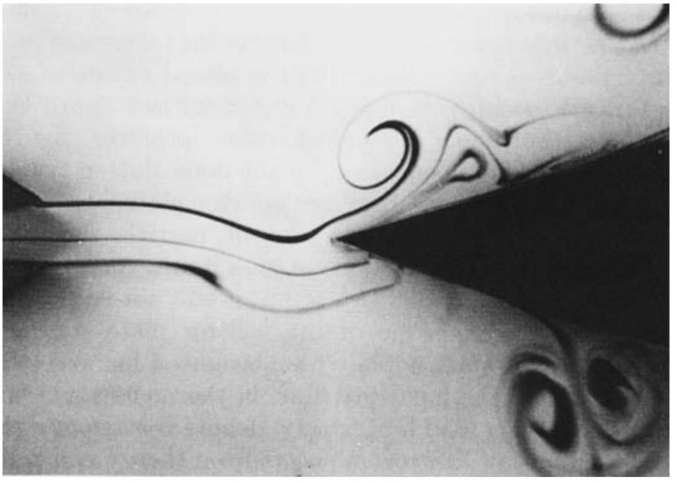

FIGURE 3. A typical edge-tone experiment, with visualization by dye injection (from Staubli & Rockwell 1987, by kind permission of the authors). Note that in this experiment the shear layers of the jet remain continuous upstream of the splitter plate, as in the modelling of this paper. In other circumstances (e.g. when the splitter plate oscillates transversely, as also studied by Staubli & Rockwell 1987) the jet shear layers may break up into vortex-street concentrations before reaching the splitter-plate edge.

order to comply with the Kutta condition, we have (§6) to add an eigensolution for the nozzle–jet interaction problem which allows the release of vorticity into the flow – and as this vorticity becomes decoupled from the nozzle, it is recognized as the sinuous instability mode with which the calculation began. Identifying it as such leads to the dispersion relation (1.1), of which we select the phase content (1.2). This is analysed in §8, §7 having given an approach to the asymptotic factorization of Wiener–Hopf kernels which we believe may be of general usefulness and which here enables the analytical approach to be followed right through, despite the presence of apparently hopelessly intractable Wiener–Hopf kernels. All the general features of the edge-tone are seen to be reproduced by the analytical predictions, and indeed the only discrepancies lie in purely numerical factors which are in part related to differences between the model and typical experiments in respect of nozzle and wedge geometry, and in part to the fact, explained in §8, that low-frequency asymptotics for spatially unstable modes give accurate results only at very low frequencies, whereas the corresponding ones for the (generally irrelevant) temporally unstable modes have a much wider range of validity.

Possible effects arising from the introduction of displacement thickness fluctuations in the boundary layers over the splitter plate, and the application of a Kutta condition at the leading edge of that plate, are discussed in §9. The paper ends with a brief discussion of other aspects calling for comment and further study.

2. Formulation

We start by writing down the exact form of the boundary-value problem for incompressible flow. A two-dimensional problem will be considered, with flow in the (x, y)-plane. A parallel plate duct $\{y = \pm b, -\infty < x < 0\}$ carries uniform inviscid incompressible flow at speed U_0. The flow emerges from the duct to form vortex sheets whose mean locations are $\{y = \pm b, 0 < x < \infty\}$, and the top-hat jet thus formed is assumed to spontaneously develop a sinuous mode of spatial instability at a real frequency ω, the time-dependent fields having the factor $\exp(-\mathrm{i}\omega t)$ which will be suppressed throughout. A rigid splitter plate is placed symmetrically in the flow, at a stand-off distance h, occupying $\{y = 0, h < x < \infty\}$ (see figure 1).

We wish to solve the linear boundary-value problem for time-harmonic perturbations, posed by Laplace's equation for the potentials in the fluid, with rigid wall conditions on the duct plates and on the splitter plate, and with vortex-sheet conditions of the continuity of pressure and of particle displacement on the continuations of the duct walls. As explained in §1, a Kutta condition will be imposed at the edges $\{x = 0, y = \pm b\}$ of the duct walls, but it will not be possible to impose a similar condition at the leading edge of the splitter plate (unless displacement thickness fluctuations on the splitter plate are accounted for; see §9).

Denote the potentials, for the unsteady flow, in the regions $y > b$, $-b < y < +b$, $y < -b$, by u, v, w, respectively, and let $\zeta(x), \eta(x)$ denote the displacements (of course with $\exp(-\mathrm{i}\omega t)$ understood) of the vortex sheets from their mean positions $y = \pm b$. Then the full boundary-value problem is defined by

$$\nabla^2(u, v, w) = 0, \tag{2.1}$$

$$\left.\begin{aligned} \frac{\partial u}{\partial y} = \frac{\partial v}{\partial y} = 0 \quad (y = +b, -\infty < x < 0), \\ \frac{\partial w}{\partial y} = \frac{\partial v}{\partial y} = 0 \quad (y = -b, -\infty < x < 0), \end{aligned}\right\} \tag{2.2}$$

$$\frac{\partial v}{\partial y} = 0 \quad (y = 0, h < x < \infty), \tag{2.3}$$

$$\left.\begin{aligned} -\mathrm{i}\omega u = \left(-\mathrm{i}\omega + U_0\frac{\partial}{\partial x}\right)v \quad (y = +b, 0 < x < \infty), \\ -\mathrm{i}\omega w = \left(-\mathrm{i}\omega + U_0\frac{\partial}{\partial x}\right)v \quad (y = -b, 0 < x < \infty) \end{aligned}\right\} \tag{2.4}$$

((2.4) expressing continuity of pressure across the vortex sheets), and

$$\left.\begin{aligned} \frac{\partial u}{\partial y} = -\mathrm{i}\omega\zeta, \quad \frac{\partial v}{\partial y} = \left(-\mathrm{i}\omega + U_0\frac{\partial}{\partial x}\right)\zeta \quad (y = +b, 0 < x < \infty), \\ \frac{\partial w}{\partial y} = -\mathrm{i}\omega\eta, \quad \frac{\partial v}{\partial y} = \left(-\mathrm{i}\omega + U_0\frac{\partial}{\partial x}\right)\eta \quad (y = -b, 0 < x < \infty) \end{aligned}\right\} \tag{2.5}$$

(which express continuity of particle displacement). The Kutta condition requires $|\nabla(u, v)| = O(1)$ as the edge $(0, +b)$ is approached, and $|\nabla(w, v)| = O(1)$ near $(0, -b)$.

We must allow exponential growth downstream of the splitter plate edge, and must also tolerate singularities in pressure and in velocity ∇v of the inverse square-root kind at the splitter-plate edge. The issue of *causality* will be discussed briefly in §10.

There is no general method for solving problems of the above kind (essentially three-part boundary-value problems with different conditions in $-\infty < x < 0$, $0 < x < h$ and $h < x < \infty$), though it is possible that a development of the ingenious technique of Möhring (1978) might lead to an exact solution. Möhring did in fact apply this method to a three-part problem involving a duct and splitter plate, and Durbin (1984) extended the calculation to demonstrate existence of discrete frequency oscillations, but the edge-tone problem appears to be significantly more complicated, involving, as it does, two vortex sheets rather than the single sheet in the problems so far discussed by Möhring. We have so far been unable to make the necessary extension and instead will tackle the problem asymptotically. In the first place, the stand-off distance h may be taken as large, the ratio $h/2b$ being normally greater than about 5 and often as high as 30. Second, the Strouhal number $St = f2b/U_0 = \omega b/\pi U_0$ is invariably low, being perhaps as small as 0.05 and never larger than 0.5. Correspondingly, the wavelength λ_0 of the hydrodynamic instability waves on the jet is larger than the duct width $2b$ (between 1.5 and 6 times the duct width, say), but considerably less than the stand-off distance h. We shall therefore seek an asymptotic solution under the restrictions

$$b \ll \lambda_0 \ll h, \tag{2.6}$$

and the way in which these inequalities are used will be evident in the subsequent analyses.

We continue in §3 with examination of the two-part problem in which an incident instability wave interacts with the splitter plate, the (distant) upstream duct being ignored. This standard two-part problem can be solved by the Wiener–Hopf method, in which the restriction $b \ll \lambda_0$ (equivalent to $St \to 0$) allows a relatively simple Wiener–Hopf factorization to be achieved. As part of the solution we obtain in §4 the field 'fed back' to large distances upstream. This field then features in §5 as the forcing for another two-part problem, in which we examine the jet interaction with the duct, ignoring the downstream splitter plate. A suitable eigensolution has to be included in the solution of this duct exit problem in order that a Kutta condition can be satisfied when the jet is forced by the feedback signal. Part of this eigensolution is a spatial instability wave, and we complete the cycle in §6 by identifying that wave with the incident instability wave of §3. This is a linear problem with no external forcing, and therefore in the identification an arbitrary amplitude factor cancels out, leaving us with the dispersion equation of the form (1.1). From this, as argued in §1, only the phase content (1.3) will be regarded as significant, and will be used to calculate the possible frequencies of operation.

3. The splitter-plate problem

Far downstream of the splitter edge, in $y > 0$,

$$u = A\exp(-\mathrm{i}\alpha x - \gamma_\alpha y), \qquad v = B\exp(-\mathrm{i}\alpha x)\cosh\gamma_\alpha y, \tag{3.1}$$

are appropriate potentials, where $\gamma_\alpha = (\alpha^2)^{\frac{1}{2}}$ with $\mathrm{Re}\,\gamma_\alpha > 0$. Applying the vortex-sheet conditions of (2.4) and (2.5) at $y = b$ gives the relation

$$A/B = D_\alpha \exp(\gamma_\alpha b)\cosh\gamma_\alpha b, \tag{3.2}$$

where $D_\alpha = 1+\alpha U_0/\omega$, provided α satisfies the dispersion relation for a varicose (symmetric, breathing) mode,

$$1+D_\alpha^2\coth\gamma_\alpha b = 0. \tag{3.3}$$

In $y < 0$ we have similarly, as $x \to +\infty$,

$$v = C\exp(-\mathrm{i}\alpha x)\cosh\gamma_\alpha y, \qquad w = D\exp(-\mathrm{i}\alpha x + \gamma_\alpha y), \tag{3.4}$$

where D/C has the same value as provided by (3.2) for A/B, and where again α satisfies (3.3). As regards (3.3), this has – at any rate in the low-Strouhal-number limit of interest here – a zero at $\alpha = -\alpha_1 + \mathrm{i}\alpha_2$, where $\alpha_1, \alpha_2 > 0$, and also one at α^*, these corresponding, respectively, to spatially amplifying and decaying modes. Approximate forms for α_1, α_2 will be given in § 7; for the moment no specific forms are needed.

The relation between the coefficients B and C, giving the pressure jump across the plate, will be determined in a moment, and then (3.2) determines A, and similarly, D. To find this relation, we consider the splitter-plate problem in the absence of the (far upstream) duct, writing $x = X+h$, and expressing the total potentials for the semi-infinite splitter plate as

$$u_{\mathrm{tot}} = A\exp(-\mathrm{i}\alpha X - \gamma_\alpha y) + u(X,y) \quad (y > b), \tag{3.5}$$

with similar expressions for the other potentials as sums of the primary fields just discussed, and which must dominate as $X \to +\infty$, plus correction potentials ϕ, ψ and w in the regions $0 < y < b$, $-b < y < 0$, $y < -b$, respectively. These correction functions are all harmonic, and satisfy $\partial\phi/\partial y = \partial\psi/\partial y = 0$ on the splitter plate $\{y = 0, 0 < X < \infty\}$. On the upstream continuation of the splitter plate, the fields and all their derivatives must be continuous, so that

$$\phi + B\,\mathrm{e}^{-\mathrm{i}\alpha X} = \psi + C\,\mathrm{e}^{-\mathrm{i}\alpha X} \quad \text{and} \quad \frac{\partial\phi}{\partial y} = \frac{\partial\psi}{\partial y} \tag{3.6}$$

for $\{y = 0, -\infty < X < 0\}$. On $\{y = \pm b, -\infty < X < +\infty\}$ the vortex-sheet conditions of § 2 must be satisfied, and they must be satisfied by the correction functions because they are already satisfied by the primary fields with coefficients (A, B, C, D).

The problem posed above is essentially a standard two-part boundary-value problem which can be solved exactly by the Wiener–Hopf technique. Before giving the solution, we express the correction fields (u, ϕ, ψ, w) as the sum of parts even in y and odd in y. Then we observe that the even part has zero y-derivative on $\{y = 0, -\infty < X < +\infty\}$, and it is therefore an eigenmode for the doubly infinite jet problem with even symmetry about $y = 0$, and as such is already included in the *primary* fields in (3.5) – which form the general such eigenmode which is finite as $X \to -\infty$. We can therefore proceed on the assumption that the *correction* fields are odd functions of y (though not necessarily continuous across $y = 0$), but we do not yet assume that the *primary* fields are odd in y.

Define transforms by

$$U(k,y) = \int_{-\infty}^{+\infty} u(X,y)\,\mathrm{e}^{\mathrm{i}kX}\,\mathrm{d}X,$$

etc., and $U_\pm(k,y)$ for the transforms of $u(X,y)H(\pm X)$. Then Laplace's equation is satisfied by

$$\left.\begin{aligned} U(k,y) &= U(k)\,\mathrm{e}^{-\gamma y}, \quad W(k,y) = -U(k)\,\mathrm{e}^{\gamma y}, \\ \Phi(k,y) &= P(k)\cosh\gamma y + Q(k)\sinh\gamma y, \quad \Psi(k,y) = -P(k)\cosh\gamma y + Q(k)\sinh\gamma y, \end{aligned}\right\} \tag{3.7}$$

in which $\gamma \equiv \gamma_k = k\,\mathrm{sgn}\,\mathrm{Re}\,k$, these solutions also being odd in y and finite as $|y| \to \infty$. Application of the vortex-sheet boundary conditions (for all X) followed by elimination of $U(k)$ gives

$$P(k)\,(D_k\cosh\gamma b + D_k^{-1}\sinh\gamma b) + Q(k)\,(D_k\sinh\gamma b + D_k^{-1}\cosh\gamma b) = 0, \tag{3.8}$$

in which $D_k = 1 + kU_0/\omega$.

This equation is essentially the Wiener–Hopf equation required, for that equation might be expected to relate the pressure drop across the plate, proportional to

$D_+(k,0) = \Phi_+(k,0) - \Psi_+(k,0)$, to the velocity $\Phi'_-(k,0)$ on the upstream extension of the plate, and we readily find

$$2P(k) = D_+(k,0) + \frac{\mathrm{i}(B-C)}{k-\alpha}, \tag{3.9}$$

$$Q(k) = \gamma^{-1}\Phi'_-(k,0) \tag{3.10}$$

(the prime indicating $\partial/\partial y$), so that (3.8) gives

$$D_+(k,0) + (2b)\,H(k)\,\Phi'_-(k,0) + \frac{\mathrm{i}(B-C)}{k-\alpha} = 0. \tag{3.11}$$

The kernel of this functional equation is

$$H(k) \equiv \frac{\coth \gamma b}{\gamma b}\,\frac{1+D_k^2 \tanh \gamma b}{1+D_k^2 \coth \gamma b}. \tag{3.12}$$

Formal solution of the Wiener–Hopf problem is standard (at any rate for real ω – we comment in §10 on complex ω and the causality issue). As $k \to \pm\infty, H(k) \sim |k|^{-1}$, so that we can define a factorization

$$H(k) = H_+(k)\,H_-(k), \tag{3.13}$$

in which $H_\pm(k)$ are analytic and non-zero in upper and lower half-planes which may (with the implicit inclusion of small dissipation, such that $\gamma_k \to (k^2+\epsilon^2)^{\frac{1}{2}}$) be taken to overlap in a strip of finite width and include the real k-axis. The factors $H_\pm(k)$ are each $O(k^{-\frac{1}{2}})$ as $|k| \to \infty$ in appropriate half-planes. Explicit forms for these factors will be given in §7; for the moment we continue formally. Then the usual arguments lead to solutions of (3.11) in the forms

$$\left.\begin{aligned} (2b)\,\Phi'_-(k,0)\,H_-(k) + \frac{\mathrm{i}(B-C)}{(k-\alpha)\,H_+(\alpha)} &= E(k), \\ \frac{D_+(k,0)}{H_+(k)} + \frac{\mathrm{i}(B-C)}{k-\alpha}\left(\frac{1}{H_+(k)} - \frac{1}{H_+(\alpha)}\right) &= -E(k), \end{aligned}\right\} \tag{3.14}$$

for any entire function $E(k)$. If the potential behaves like $X^{\frac{1}{2}}$ near the plate edge (a *leading* edge) and the velocities like $X^{-\frac{1}{2}}$, it follows that $\Phi'_-(k,0) \sim k^{-\frac{1}{2}}, D_+(k,0) \sim k^{-\frac{3}{2}}$ at infinity, and hence from Liouville's theorem that

$$E(k) \equiv 0. \tag{3.15}$$

This choice of $E(k)$ gives the *least singular* solution, while (3.14) of course gives the *general* solution bounded upstream, regardless of the causality question. The least singular solution has pressure and velocity singularities of the $X^{-\frac{1}{2}}$ kind familiar in leading-edge flows, and these cannot be relieved within the present model. A singularity of this kind was removed in one of the alternatives studied by Goldstein (1981); there, however, an externally imposed forcing field (a gust or acoustic wave) *induced* a singularity, and this could then be removed by the addition of a suitable multiple of the eigensolution under study here. Howe (1981 *a*, *b*, *c*) was able to remove the same singularity, but in the absence of any external forcing, by invoking displacement thickness fluctuations in the boundary layer on the splitter plate. The boundary condition

$$\partial\phi/\partial y = \partial\psi/\partial y = 0 \quad \text{on} \quad 0 < X < \infty,$$

is replaced by his approach by

$$\partial\phi/\partial y = -\partial\psi/\partial y = V\exp(\mathrm{i}\kappa X), \tag{3.16}$$

with κ the wavenumber of a Tollmien–Schlichting wave at frequency ω, and the constant V can be determined to remove the $X^{-\frac{1}{2}}$ velocity and pressure singularity. We shall examine the consequences of introducing (3.16) later in this paper, in §9. For the present we have no displacement thickness fluctuations and no external forcing, and the leading-edge singularity therefore stays.

From (3.14) and (3.15) we find

$$U(k) = \frac{\mathrm{i}(B-C)}{2}\frac{D_k}{k-\alpha}\frac{H_+(k)}{H_+(\alpha)}\frac{\mathrm{e}^{\gamma b}}{(\cosh\gamma b)[1+D_k^2\tanh\gamma b]}, \tag{3.17}$$

a form suitable for use in the inversion integral

$$u(X,y) = \frac{1}{2\pi}\int_{-\infty}^{+\infty} U(k)\exp(-\mathrm{i}kX-\gamma y)\,\mathrm{d}k, \tag{3.18}$$

when $X < 0$, showing that the poles in the upper half-plane are at $k = \alpha$, and at the *sinuous mode instability wavenumber* $k = \beta$, where

$$1+D_\beta^2\tanh\gamma_\beta b = 0. \tag{3.19}$$

For $X > 0$ the appropriate form is

$$U(k) = \frac{\mathrm{i}(B-C)}{2}\frac{D_k}{k-\alpha}\frac{1}{H_-(k)H_+(\alpha)}\frac{\operatorname{cosech}\gamma b}{\gamma b}\frac{\mathrm{e}^{\gamma b}}{1+D_k^2\coth\gamma b}, \tag{3.20}$$

and the only pole in the lower half-plane is at $k = \alpha^*$, corresponding to the decaying varicose mode.

Consider $X < 0$ and, without loss of generality, examine the residue fields from the poles at $k = \alpha$ and $k = \beta$ on $y = b$ only. The real axis integration path in (3.18) may then be deformed over the poles at $k = \alpha, k = \beta$ onto the edges of a vertical branch cut from $k = 0+$ to $k = \mathrm{i}\infty$. The residue at $k = \alpha$ gives a contribution to $u(X,b)$ equal to

$$-\tfrac{1}{2}(B-C)D_\alpha\cosh\gamma_\alpha b\exp(-\mathrm{i}\alpha X),$$

to which we have to add the primary-mode contribution in (3.5) to obtain a total α-mode

$$u_\alpha(X,b) = [A\exp(-\gamma_\alpha b)-\tfrac{1}{2}(B-C)D_\alpha\cosh\gamma_\alpha b]\,\mathrm{e}^{-\mathrm{i}\alpha X}. \tag{3.21}$$

Now we argue that since, as will be shown in §7, the α-mode grows more slowly at low frequencies than the sinuous β-mode, it follows that as $X\rightarrow-\infty$ the field will be dominated by the α-mode (3.21) – whereas what we intend to study is the incidence on the splitter plate of a sinuous mode and its conversion, as $X\rightarrow+\infty$, into a varicose mode. The coefficient in square brackets in (3.21) must therefore vanish, and because of relation (3.2) it then follows at once that

$$B = -C, \quad A = -D, \tag{3.22}$$

and so that, if the incident instability is to be purely sinuous, the total potential field must be odd in y.

This is true in $X > 0$, of course, and shows that the emergent α-mode (3.1) is not a varicose mode for the whole jet $(-b < y < +b)$; rather, there is a varicose mode on each half-jet $(-b < y < 0, 0 < y < +b)$, as demanded by the hard-wall condition on $y = 0$, but the two varicose modes are π out of phase to comply with (3.22) and as is suggested by the vorticity concentrations of figure 3.

Having removed the α-mode in this way, we are left (apart from the branch-line integral) with the residue from the sinuous mode pole at $k = \beta$,

$$u_\beta(X, b) = B\frac{D_\beta \sinh(\gamma_\beta b)\, H_+(\beta)}{(\gamma_\alpha b)(\beta-\alpha)\, H'(\beta)\, H_+(\alpha)}\mathrm{e}^{-\mathrm{i}\beta X}. \tag{3.23}$$

Thus if we are given the amplitude (i.e. the coefficient of $\exp(-\mathrm{i}\beta X)$) of an incident β-mode, equations (3.23) and (3.2) determine the amplitude factor A of the α-mode which ultimately emerges far downstream from the edge because the solution in (3.5) for u_{tot} contains, in addition to that emergent α-mode, only an exponentially decaying residue field from the pole at $k = \alpha^*$ and an algebraically decaying field from the branch-line integral.

4. The upstream feedback field

In $X < 0$ and $Y = y - b > 0$, the appropriate form of the potential scattered by the splitter plate is, according to (3.17) and (3.18),

$$u(X, Y) = \frac{\mathrm{i}B}{2\pi}\int_{-\infty}^{+\infty} \frac{D_k}{k-\alpha}\frac{H_+(k)}{H_+(\alpha)}\frac{\exp(\mathrm{i}k|X| - \gamma Y)\,\mathrm{d}k}{(\cosh\gamma b)[1 + D_k^2 \tanh\gamma b]}, \tag{4.1}$$

and the exponential factor is $\mathrm{e}^{\mathrm{i}kZ}$ in $\mathrm{Re}\, k > 0$, and $\mathrm{e}^{\mathrm{i}kZ^*}$ in $\mathrm{Re}\, k < 0$, where $Z = |X| + \mathrm{i}Y, |X| = R\cos\Theta, 0 < \Theta < \frac{1}{2}\pi$. The real axis integration path may be deformed onto the edges of a vertical cut from 0, with $k = \mathrm{i}v, 0 < v < \infty$, on the right of the cut. Residue contributions will be ignored in the following, which concentrates on the algebraically decaying field represented by the branch-line integral. This field is

$$u_\infty = -\frac{B}{2\pi}\int_0^\infty \mathrm{d}v \frac{D_k}{k-\alpha}\frac{H_+(k)}{H_+(\alpha)}\frac{1}{\cos vb}\left(\frac{\mathrm{e}^{-vZ}}{1 + \mathrm{i}D_k^2 \tan vb} - \frac{\mathrm{e}^{-vZ^*}}{1 - \mathrm{i}D_k^2 \tan vb}\right). \tag{4.2}$$

For the e^{-vZ} term, rotate the path of the v-integration clockwise through Θ, putting $v = \zeta\mathrm{e}^{-\mathrm{i}\Theta}, 0 < \zeta < \infty$, and giving a contribution to u_∞ of

$$-\frac{B}{2\pi}\int_0^\infty \mathrm{d}\zeta \exp[-\mathrm{i}\Theta - \zeta R]\left[\left(\frac{D_k}{k-\alpha}\right)\frac{H_+(k)}{H_+(\alpha)}\frac{1}{(\cosh kb)(1 + D_k^2 \tanh kb)}\right],$$

with the contents of the square brackets evaluated at $k = \mathrm{i}\zeta\mathrm{e}^{-\mathrm{i}\Theta}$.

This integral may be evaluated asymptotically, as $R \to \infty$, by expanding the terms in the square brackets asymptotically for $\zeta \to 0$ and integrating term by term. All the terms can be trivially expanded, save for $H_+(k)$. It will appear later, when we come to the Wiener–Hopf factorization, that we can set $H_+(k) = k_+^{-\frac{1}{2}}J_+(k)$, where the cut for $k_+^{-\frac{1}{2}}$ lies in the lower half-plane, and where $J_+(0)$ is finite. Then we at once have the above contribution in the asymptotic form

$$\frac{B}{2\pi\alpha\exp(\frac{1}{4}\pi\mathrm{i} + \frac{1}{2}\mathrm{i}\Theta)}\frac{J_+(0)}{H_+(\alpha)}\int_0^\infty \zeta^{-\frac{1}{2}}\mathrm{e}^{-\zeta R}\,\mathrm{d}\zeta = \frac{B}{2\pi^{\frac{1}{2}}\alpha\,\mathrm{e}^{\frac{1}{4}\pi\mathrm{i}}}\frac{J_+(0)}{H_+(\alpha)}\frac{1}{Z^{\frac{1}{2}}}. \tag{4.3}$$

Similar treatment of the $\exp(-vZ^*)$ term in (4.2) gives a contribution

$$-\frac{B}{2\pi^{\frac{1}{2}}\alpha\,\mathrm{e}^{\frac{1}{4}\pi\mathrm{i}}}\frac{J_+(0)}{H_+(\alpha)}\frac{1}{Z^{*\frac{1}{2}}},$$

and thus
$$u_\infty \sim \frac{B}{2\pi^{\frac{1}{2}}\alpha\,\mathrm{e}^{\frac{1}{4}\pi\mathrm{i}}}\frac{J_+(0)}{H_+(\alpha)}\frac{-2\mathrm{i}\sin\frac{1}{2}\Theta}{R^{\frac{1}{2}}}. \tag{4.4}$$

In particular, for finite values of Y and large values of $|X|$,
$$u_\infty \sim \frac{B}{2\pi^{\frac{1}{2}}\alpha\,\mathrm{e}^{\frac{1}{4}\pi\mathrm{i}}}\frac{J_+(0)}{H_+(\alpha)}\frac{-\mathrm{i}Y}{|X|^{\frac{3}{2}}}, \tag{4.5}$$

and therefore, in the vicinity of the exit of the distant upstream duct, the 'upstream feedback field' takes, approximately, the form of a periodic uniform streaming flow normal to the mean flow direction,
$$u_\infty \sim Gy, \tag{4.6}$$
$$G = -\frac{\mathrm{i}BJ_+(0)}{2\pi^{\frac{1}{2}}\alpha h^{\frac{3}{2}}\mathrm{e}^{\frac{1}{4}\pi\mathrm{i}}H_+(\alpha)}. \tag{4.7}$$

A similar analysis can be conducted for the upstream feedback component ϕ_∞ of the field within the jet, $-b < y < +b$, and the same result is, naturally, found, namely $\phi_\infty \sim Gy$. The field $u_\infty = \phi_\infty = Gy$ does, of course, satisfy Laplace's equation and the necessary conditions on the vortex-sheet jet boundaries $y = \pm b$. It does not, however, satisfy the hard-wall conditions on the duct boundaries, and the next step is to consider the motion in the vicinity of the duct exit to determine the correction to (u_∞, ϕ_∞) which will enable those conditions to be satisfied – while at the same time retaining satisfaction of the conditions on the vortex sheets. The far downstream splitter plate has served to determine the forcing fields (u_∞, ϕ_∞), and no further account will be taken of the presence of the splitter plate.

5. Jet response to feedback forcing

Consider the region $y > b$ with potential u_{tot}, the region $0 < y < b$ with potential v_{tot}, and write, for the analysis of the jet exit behaviour,
$$u_{\mathrm{tot}} = Gy + u, \qquad v_{\mathrm{tot}} = Gy + \phi, \tag{5.1}$$
where G will be taken eventually to be given by (4.7). Hard-wall conditions prevail for $y = b$, $-\infty < x < 0$, vortex-sheet conditions for $y = b, 0 < x < \infty$, and the splitter plate is ignored. The problem for the perturbation potentials is therefore defined by
$$\nabla^2\begin{pmatrix} u \\ \phi \end{pmatrix} = 0, \tag{5.2}$$
$$\frac{\partial u}{\partial y} = \frac{\partial \phi}{\partial y} = -G \quad \text{on} \quad \{y = b, -\infty < x < 0\}, \tag{5.3}$$
$$\phi = 0 \quad \text{on} \quad y = 0, \quad \text{all } x, \tag{5.4}$$
$$\left.\begin{aligned} \left(-\mathrm{i}\omega + U_0\frac{\partial}{\partial x}\right)\frac{\partial u}{\partial y} &= -\mathrm{i}\omega\frac{\partial \phi}{\partial y} \\ -\mathrm{i}\omega u &= \left(-\mathrm{i}\omega + U_0\frac{\partial}{\partial x}\right)\phi \end{aligned}\right\} \quad \text{on} \quad \{y = b, 0 < x < \infty\}. \tag{5.5a, b}$$

Now the lack of decay of the forcing term $(-G)$ in (5.3) makes it impossible to solve the problem as posed. Difficulties of this kind are familiar in half-plane problems involving Laplace's equations (see, for example, Noble 1958, pp. 139–140; Orszag &

Crow 1970) and they may be circumvented in a number of ways. The correct way is to recognize that the potential Gy is only a local approximation, the more accurate form (4.4) or (4.5) decaying as $x \to -\infty$.

We shall shortly carry out the calculation for a uniformly valid approximation to the feedback forcing field. First, however, we modify (5.3) slightly, in a way that leads to a well-posed problem and in a way that permits rapid generalization to deal with the uniform approximation to the forcing.

We propose to replace (5.3) by

$$\frac{\partial u}{\partial y} = \frac{\partial \phi}{\partial y} = -G\,\mathrm{e}^{\epsilon x} \quad \text{on} \quad \{y = b, -\infty < x < 0\}, \tag{5.6}$$

where ϵ is real and positive. This retains the physical character of the upstream forcing near the duct exit, and cuts off the forcing over a large upstream length ϵ^{-1} *with no phase change*, this conveniently representing a variety of effects of which it may not be feasible to take full account. The value of ϵ (small) does not enter into the relations for the feedback cycle frequencies provided ϵ is taken as real; thus all phase changes are associated with the vortical parts of the cycle only – the instability interaction with the splitter plate and the vortex shedding from the duct exit – and not with the incompressible irrotational upstream feedback. Analysis using a uniformly valid representation of the upstream feedback field does in fact lead precisely to the same results as (5.6), with an appropriate real ϵ, as we shall see later, in §7.

With the replacement of (5.3) by (5.6), it is straightforward to come to the Wiener–Hopf equation

$$U'_+(k,b) + \frac{\mathrm{i}G}{k - \mathrm{i}\epsilon} = K(k)\,F_-(k), \tag{5.7}$$

in which

$$\left.\begin{aligned} U'_+(k,b) &= \int_0^\infty \mathrm{e}^{\mathrm{i}kx} \frac{\partial u}{\partial y}(x,b)\,\mathrm{d}x, \\ F_-(k) &= D_k\,\Phi_-(k,b) - U_-(k,b) + \mathrm{i}\frac{U_0}{\omega}\phi_0, \end{aligned}\right\} \tag{5.8}$$

ϕ_0 is the finite value of $\phi(0,b)$, and

$$K(k) = \frac{\gamma}{1 + D_k^2 \tanh \gamma b} = \frac{\gamma}{M(k)}, \tag{5.9}$$

the kernel here involving only the dispersion function appropriate to the sinuous mode, as would be expected from the nature of the forcing. In terms of a factorization

$$K(k) = K_+(k)\,K_-(k),$$

with $K_\pm(k) = O(k^{-\frac{1}{2}})$ at infinity, the solution of (5.7) with the minimal level of singularity is

$$U'(k,b) = \frac{\mathrm{i}GK_+(k)}{(k - \mathrm{i}\epsilon)\,K_+(\mathrm{i}\epsilon)}. \tag{5.10}$$

This is composed of a contribution

$$U'_-(k,b) = \frac{\mathrm{i}G}{k - \mathrm{i}\epsilon}$$

associated with the feedback forcing, and a contribution

$$U'_+(k,b) = -\frac{\mathrm{i}G}{k-\mathrm{i}\epsilon}\left(1-\frac{K_+(k)}{K_+(\mathrm{i}\epsilon)}\right), \tag{5.11}$$

which is $O(k^{-\frac{3}{2}})$ at infinity in the upper half-plane. The corresponding value of $\partial u/\partial y$ is then $O(r^{\frac{1}{2}})$, where r is the distance to the duct edge $(0,b)$, and (5.5*a*) then shows that $\partial\phi/\partial y$ is singular, like $O(r^{-\frac{1}{2}})$. This velocity singularity in the moving jet fluid will be eliminated in a moment. For the present, we note that the part of $U'(k,b)$ which leads to a singularity is

$$\frac{\mathrm{i}G}{K_+(\mathrm{i}\epsilon)}\frac{K_+(k)}{k}. \tag{5.12}$$

Now return to (5.1) and replace the local cross-stream forcing potential by an exact (or uniformly valid asymptotic) expression. Thus we write

$$u_{\text{tot}} = u_\infty + u, \quad v_{\text{tot}} = v_\infty + v, \quad \eta_{\text{tot}} = \eta_\infty + \eta, \tag{5.13}$$

where the forcing fields $(u_\infty, v_\infty, \eta_\infty)$ satisfy the vortex-sheet conditions at $y = +b$ for all x, and η refers to the deflection from $y = +b$ of that vortex sheet. Then (5.3) is modified accordingly, but a Wiener–Hopf equation

$$U'_+(k,b) + \mathrm{i}\omega Z_-(k) = K(k)F_-(k) \tag{5.14}$$

can be derived as before, in which $U'_+(k,b)$, $F_-(k)$ and $K(k)$ are as defined in (5.8) and (5.9), and the forcing function replacing $\mathrm{i}G/(k-\mathrm{i}\epsilon)$ in (5.7) is $\mathrm{i}\omega Z_-(k)$, where

$$Z_-(k) = \int_{-\infty}^{0} \eta_\infty(x)\,\mathrm{e}^{\mathrm{i}kx}\,\mathrm{d}x.$$

However, we have, from (4.2), an expression for $u_\infty(X,Y)$ from which η_∞ can be calculated, and we find that

$$-\mathrm{i}\omega\eta_\infty = \int_0^\infty G(\zeta)\,\mathrm{e}^{\zeta x}\,\mathrm{d}\zeta \tag{5.15}$$

for $-\infty < x < 0$, where

$$G(\zeta) = \frac{B}{2\pi}\left[\frac{\mathrm{e}^{-\zeta h}D_k}{(k-\alpha)}\frac{J_+(k)}{H_+(\alpha)}\left(\frac{k^{\frac{1}{2}}}{\cosh kb}\right)\{(1+D_k^2\tanh kb)^{-1} + (1-D_k^2\tanh kb)^{-1}\}\right]_{k=\mathrm{i}\zeta}. \tag{5.16}$$

Observe that as $h\to\infty$,

$$-\mathrm{i}\omega\eta_\infty \sim \frac{B}{2\pi}\frac{\mathrm{e}^{\frac{1}{4}\pi\mathrm{i}}}{(-\alpha)}\frac{J_+(0)}{H_+(\alpha)}2\int_0^\infty \zeta^{\frac{1}{2}}\exp\left[-\zeta(h+|x|)\right]\mathrm{d}\zeta = \left(\frac{B}{2\pi}\frac{\mathrm{e}^{\frac{1}{4}\pi\mathrm{i}}}{\alpha}\right)\frac{2J_+(0)}{H_+(\alpha)}\frac{\frac{1}{2}!}{(h+|x|)^{\frac{3}{2}}}, \tag{5.17}$$

uniformly in $|x|$. For $|x| \ll h$ this gives a constant value for η_∞ which agrees with that which follows from (4.6) and (4.7). It is the form of (5.15) which is particularly convenient, however. All we have to do is to replace G in the result (5.11) by $G(\zeta)$, ϵ by ζ and carry out $\int_0^\infty \mathrm{d}\zeta$, and then the effects of forcing by the upstream feedback field will be fully accounted for. The integral for ζ can be carried out asymptotically as $h\to\infty$. We do this when the dispersion equation has been derived, and in the meantime we continue with the simple expression (5.11).

The singular solution obtained in this way is the only possible solution which is bounded as $x\to+\infty$ (and therefore possesses a Fourier transform). To alleviate the singularity we have to find a solution *unbounded* as $x \rightarrow +\infty$. Following Orszag & Crow (1979) and Crighton (1972), we do this by extracting the unbounded part of the solution, and this must necessarily take the form of a sinuous freely developing instability β-mode (the α-mode can be excluded, as it could not lead to a field capable of cancelling the antisymmetric singularities at $y = \pm b, x = 0$). Write the total potentials (leaving aside the feedback forcing altogether, and considering only the spontaneous development of a sinuous instability on the jet as it emerges from the duct) in the forms

$$u_{\text{tot}} = A_1 \exp(-\mathrm{i}\beta x - \gamma_\beta y) + u, \qquad v_{\text{tot}} = B_1 \exp(-\mathrm{i}\beta x) \sinh \gamma_\beta y + \phi, \tag{5.18}$$

where
$$A_1/B_1 = D_\beta \mathrm{e}^{\gamma_\beta b} \sinh \gamma_\beta b \quad \text{and} \quad 1 + D_\beta^2 \tanh \gamma_\beta b = 0 \tag{5.19}$$

(cf. (3.2) and (3.3) for the varicose α-mode). The first terms in (5.18) act as forcing for another Wiener–Hopf problem, for which the functional equation is

$$U'_+(k, b) - \frac{\mathrm{i}\gamma_\beta A_1 \mathrm{e}^{-\gamma_\beta b}}{k - \beta} = K(k) F_-(k), \tag{5.20}$$

with the definitions of (5.8) and (5.9). The minimally singular solution of (5.20) is

$$U'_+(k, b) = \frac{\mathrm{i}\gamma_\beta A_1 \mathrm{e}^{-\gamma_\beta b}}{k - \beta} \left\{1 - \frac{K_+(k)}{K_+(\beta)}\right\}, \tag{5.21}$$

and the part of this leading to singular velocities in the jet fluid at the duct edges is, as in (5.12),

$$-\frac{\mathrm{i}\gamma_\beta A_1 \mathrm{e}^{-\gamma_\beta b}}{K_+(\beta)} \left\{\frac{K_+(k)}{k}\right\}. \tag{5.22}$$

For the moment, this completes the study of the duct-exit problem, though we shall return to the solutions given here later, for discussion of the phase changes occurring in various parts of the feedback cycle.

6. The Kutta condition and the dispersion relation

We now add a suitable 'eigensolution' (5.18) to the forced solution (5.1) driven by the upstream feedback, choosing the constant A_1 so that the complete solution has finite velocities in the neighbourhood of each of the edges ($x = 0, y = \pm b$). This requires, from (5.12) and (5.22), that

$$\frac{\mathrm{i}G}{K_+(\mathrm{i}\epsilon)} - \frac{\mathrm{i}\gamma_\beta A_1 \mathrm{e}^{-\gamma_\beta b}}{K_+(\beta)} = 0. \tag{6.1}$$

This relation, arising from the satisfaction of a Kutta condition (Crighton 1985) at each of the duct trailing edges, is, in turn, just the dispersion relation for the operating stages of the edge-tone, for

$$A_1 \exp(-\mathrm{i}\beta h) \exp\{-\mathrm{i}\beta X - \gamma_\beta y\}$$

is the potential outside the jet of the sinuous β-mode, whose interaction with the splitter plate was examined in §3, and (3.23) gives another expression for this potential, from which we have

$$A_1 \exp(-\mathrm{i}\beta h) = B \frac{D_\beta \sinh(\gamma_\beta b) H_+(\beta) \mathrm{e}^{\gamma_\beta b}}{\gamma_\beta b(\beta - \alpha) H'(\beta) H_+(\alpha)}.$$

When this value of A_1 and (4.7) for G are inserted into (6.1), the arbitrary amplitude factor cancels, and we have

$$\frac{e^{\frac{1}{4}\pi i}J_+(0)}{2\pi^{\frac{1}{2}}\alpha h^{\frac{3}{2}}K_+(i\epsilon)}+\frac{e^{i\beta h}D_b\sinh(\gamma_\beta b)\,H_+(\beta)}{K_+(\beta)\,b(\beta-\alpha)\,H'(\beta)}=0. \tag{6.2}$$

The properties of this dispersion relation will be discussed in §8, where appropriate simplifications will be made. These depend, of course, on details of the various factorizations which will be obtained in the next section. It might have been expected that such details would be relegated to an Appendix, rather than the argument allowed to be interrupted by what may be thought to be issues of mathematical technique only. We believe, however, that these details should be included here in the main text, as they illuminate the physics, and are obtained by what we consider to be a novel approach, giving a significant improvement over existing techniques and of wide applicability in the analysis of unsteady fluid mechanics problems.

7. Wiener–Hopf factorizations by matched asymptotic expansions

The Wiener–Hopf kernels occurring in this problem are extremely complicated, and the exact Cauchy integral expressions for the factorizations are not useful (though they could be computed – perhaps after some preliminary contour deformation – for any particular case of interest). It is therefore natural to turn to the question of approximate factorization, for which at present there seem to be two established techniques.

The first, due to Carrier and Koiter (see Noble 1958, p. 160), advocates the replacement of a complicated kernel by one which approximates it reasonably on the real k-axis (though not necessarily elsewhere in the k-plane) and which can be readily factorized. As the simplest example, $\exp(-k^2)$ is not immediately factorizable, but we might hope that it can be sufficiently well approximated by $(k^2+1)^{-1}$ on the real axis, in which case the multiplicative split into factors $(k\pm i)^{-1}$, analytic and non-zero in overlapping upper and lower half-planes, is immediate. The disagreement between $\exp(-k^2)$ and $(k^2+1)^{-1}$ off the real axis is irrelevant, because the Cauchy integrals defining the split functions involve only values of the kernel on the real axis. The principal argument against the Carrier–Koiter method is that no criterion – other than of pragmatism or aesthetics – is used to decide when a function can be adequately approximated by another for this purpose.

In the second method, due to Kranzer & Radlow (1962, 1965), one exploits the presence of a small parameter, S, say, and seeks approximations to the factors $K_\pm(k,S)$ which are asymptotic to the exact factors as $S\to 0$. This procedure, although established rigorously for certain classes of kernel $K(k,S)$, is of extremely limited applicability. Suffice it to say here that the kernel is required to contain S in the explicit form $K(k,S)=K_0(k)+SK_1(k)$ and that the asymptotic factorizations $K_\pm(k,S)$ are valid only for $O(1)$ values of k, and not for the large values of k from which edge behaviour can be ascertained (as in §5 here, for example). The small parameter which we use here as the basis for asymptotics is the frequency parameter $\omega b/U_0=S$, but our kernels do not contain S in the simple explicit manner of Kranzer & Radlow, nor can they be uniformly so approximated.

We propose here to achieve the factorization by the use of matched asymptotic expansions (MAE). There are several slightly different ways in which MAE can be used here, and the most convenient is really to use MAE as the criterion for replacement of a complicated kernel by a simpler one, as in the Carrier–Koiter method. We shall approximate our kernels uniformly, as $S \to 0$, over the whole of the real k-axis, with a sequence of overlapping approximations, from which we can form a uniformly valid multiplicative composite kernel. Most of the terms in this multiplicative composite can be factorized at sight, and we need Cauchy integrals (or equivalent) for only one term – and there we are faced with a purely numerical problem from which all S-dependence has been scaled out, and which in any case we are able to solve completely in analytical form.

The kernel $H(k)$ of (3.12) is

$$H(k) = K(k)M(k)/N(k),$$

with

$$L(k) = (\coth \gamma b)/\gamma b, \tag{7.1}$$

$$M(k) = 1+D_k^2 \tanh \gamma b, \tag{7.2}$$

$$N(k) = 1+D_k^2 \coth \gamma b, \tag{7.3}$$

and $\gamma = k$ for $\operatorname{Re} k > 0, \gamma = -k$ for $\operatorname{Re} k < 0$. We define the obvious dimensionless wavenumbers

$$\sigma = kb, \quad \tau = kU_0/\omega = \sigma/S, \tag{7.4}$$

with $S = \omega b/U_0 \ll 1$. Then

$$L = \frac{\coth (\sigma^2)^{\frac{1}{2}}}{(\sigma^2)^{\frac{1}{2}}} = \frac{\coth \sigma}{\sigma} \tag{7.5}$$

(where we write $(\sigma^2)^{\frac{1}{2}}$ for σ or $-\sigma$ according as $\operatorname{Re}\sigma \gtrless 0$).

For $M(k)$, take $\sigma = O(1)$ and let $S \to 0$. Then

$$M(\sigma) = 1+\left(1+\frac{\sigma}{S}\right)^2 \tanh (\sigma^2)^{\frac{1}{2}} \sim \frac{\sigma^2}{S^2}\tanh (\sigma^2)^{\frac{1}{2}}. \tag{7.6}$$

This approximation to M in fact has *no overlap* with the corresponding approximation obtained by holding $\tau = O(1)$ in M and letting $S \to 0$. It turns out that it is necessary to introduce the new scaled wavenumber q according to

$$\sigma = S^{\frac{2}{3}}q, \tag{7.7}$$

and then

$$M(q) = 1+\left[1+\frac{q}{S^{\frac{1}{3}}}\right]^2 \tanh [S^{\frac{2}{3}}(q^2)^{\frac{1}{2}}] \sim 1+q^2(q^2)^{\frac{1}{2}}, \tag{7.8}$$

as $S \to 0, q = O(1)$. Evidently (7.6) and (7.8) do overlap, as $\sigma \to 0$ and $q \to \infty$, respectively, with common value $q^2(q^2)^{\frac{1}{2}}$, while (7.8) is evidently good down to $q = 0$ and makes the introduction of τ unnecessary. A multiplicative composite approximation to M then follows as

$$M \sim \frac{\tanh \sigma}{\sigma}[1+q^2(q^2)^{\frac{1}{2}}], \tag{7.9}$$

valid for all real wavenumbers.

For $N(k)$, the scaled wavenumber q is redundant and approximations for $\sigma = O(1)$ and $\tau = O(1)$ overlap and cover the whole real wavenumber range. In terms of σ,

$$N = 1+\left[1+\frac{\sigma}{s}\right]^2 \coth (\sigma^2)^{\frac{1}{2}} \sim \frac{\sigma^2}{S^2}\coth (\sigma^2)^{\frac{1}{2}}, \tag{7.10}$$

while in terms of τ,

$$N = 1+(1+\tau)^2 \coth S(\tau^2)^{\frac{1}{2}},$$

which can be approximated by

$$(1+\tau)^2/S(\tau^2)^{\frac{1}{2}}$$

except near $\tau = -1$. One finds that

$$N(\tau) \sim \frac{1}{S(\tau^2)^{\frac{1}{2}}}\{S+(1+\tau)^2\} \tag{7.11}$$

is uniformly good for $\tau = O(1)$, including τ close to -1 and, further, that (7.10) and (7.11) overlap as $\sigma \to 0$ and $\tau \to \infty$, with common value $(\sigma^2)^{\frac{1}{2}}S^{-2}$. Thus the multiplicative composite approximation to $N(k)$ is

$$N(k) \sim \frac{\sigma \coth \sigma}{(\sigma^2)^{\frac{1}{2}}}\{S+(1+\tau)^2\}. \tag{7.12}$$

From (7.5, (7.9) and (7.12) we thus come to the uniformly valid approximate description of $H(k)$, on the real axis, as $S \to 0$,

$$H(k) \sim \frac{\tanh \sigma}{\sigma}\frac{1}{(\sigma^2)^{\frac{1}{2}}}(1+q^2(q^2)^{\frac{1}{2}})\frac{1}{S+(1+\tau)^2}. \tag{7.13}$$

Approximations to the instability wavenumbers follow at once. For the varicose mode the function $N(k)$ is relevant, and we have

$$\alpha \sim (\omega/U_0)(-1+\mathrm{i}S^{\frac{1}{2}}), \tag{7.14}$$

while for the sinuous mode $M(k)$ is relevant, and

$$\beta \sim (\omega/U_0)S^{-\frac{1}{3}}(-\tfrac{1}{2}+\mathrm{i}\tfrac{1}{2}\surd 3). \tag{7.15}$$

Observe, as was claimed in §3, that the varicose mode grows much more slowly, as $S \to 0$, than the sinuous.

Factorization of much of (7.13) is now immediate. We have (e.g. Noble 1958, p. 41)

$$\frac{\tanh \sigma}{\sigma} \equiv \frac{[-\frac{1}{2}-\mathrm{i}\sigma/\pi]!}{\pi^{\frac{1}{2}}[-\mathrm{i}\sigma/\pi]!}\frac{[-\frac{1}{2}+\mathrm{i}\sigma/\pi]!}{\pi^{\frac{1}{2}}[\mathrm{i}\sigma/\pi]!}, \tag{7.16}$$

in which the indicated factors are analytic and non-zero in $\operatorname{Im}\sigma > -\frac{1}{2}\pi$, $\operatorname{Im}\sigma < +\frac{1}{2}\pi$ respectively, and are each $O(\sigma^{-\frac{1}{2}})$ as $|\sigma| \to \infty$ therein. Second,

$$\frac{1}{(\sigma^2)^{\frac{1}{2}}} \equiv \frac{1}{(\sigma+\mathrm{i}0)^{\frac{1}{2}}}\frac{1}{(\sigma-\mathrm{i}0)^{\frac{1}{2}}} \tag{7.17}$$

with branch cuts from $\mp \mathrm{i}0$ to $\mp \mathrm{i}\infty$, respectively. Third

$$S+(1+\tau)^2 \equiv (\tau+1+\mathrm{i}S^{\frac{1}{2}})(\tau+1-\mathrm{i}S^{\frac{1}{2}}), \tag{7.18}$$

the factors corresponding to decaying and amplifying varicose instability modes, respectively.

The factorization of

$$R(q) = 1+q^2(q^2)^{\frac{1}{2}}$$

is more complicated. For the moment let q be real, so that $(q^2)^{\frac{1}{2}} = |q|$. Then taking logarithms and differentiating gives (if $R(q) = R_+(q)R_-(q)$)

$$\frac{\mathrm{d}}{\mathrm{d}q}\ln R_+(q)+\frac{\mathrm{d}}{\mathrm{d}q}\ln R_-(q) = \frac{3q^5}{q^6-1}-3q^2\frac{\operatorname{sgn} q}{q^6-1}. \tag{7.19}$$

Define the zeros

$$q_1 = -q_4 = 1; \quad q_2 = -q_5 = \mathrm{e}^{\frac{1}{3}\pi\mathrm{i}}; \quad q_3 = -q_6 = \mathrm{e}^{\frac{2}{3}\pi\mathrm{i}}. \tag{7.20}$$

Then

$$\frac{\mathrm{d}}{\mathrm{d}q}\ln\left(\frac{R_+(q)}{\prod_{n=1}^{3}(q+q_n)^{\frac{1}{2}}}\right)+\frac{\mathrm{d}}{\mathrm{d}q}\ln\left(\frac{R_-(q)}{\prod_{n=1}^{3}(q-q_n)^{\frac{1}{2}}}\right)$$
$$= -3\left(\sum_{n=1}^{3}\alpha_n q_n\frac{|q|}{(q-q_n)}+\sum_{n=1}^{3}\alpha_n q_n\frac{|q|}{(q+q_n)}\right), \tag{7.21}$$

where $\alpha_n^{-1} = 6q_n^5$. Now introduce the additive decomposition of $|q|$,

$$|q| = Q_+(q)+Q_-(q), \quad Q_+(q) = \tfrac{1}{2}q+\frac{\mathrm{i}q}{\pi}\ln_+ q, \quad Q_-(q) = \tfrac{1}{2}q-\frac{\mathrm{i}q}{\pi}\ln_- q, \tag{7.22}$$

where each of $\ln_\pm 1 = 1$ and the cut for $\ln_+$ goes from 0 to $-\mathrm{i}\infty$, that for $\ln_-$ from 0 to $+\mathrm{i}\infty$. Observe that with these definitions, $Q_+(q) = Q_-(-q)$. Then the right-hand side of (7.21) may be additively decomposed in the familiar manner, after which integration and exponentiation give

$$R_+(q) = A_+\prod_{n=1}^{3}(q+q_n)^{\frac{1}{2}}\exp\left(\frac{\mathrm{i}}{\pi}\sum_{n=1}^{3}\frac{1}{q_n^2}\int_q^{\infty}\frac{\ln_+(q/q_n)}{q^2-q_n^2}\mathrm{d}q\right). \tag{7.23}$$

There is a corresponding expression for $R_-(q)$; if one wishes to have the property $R_+(-q) = R_-(q)$, then A_+ must be chosen as $\exp(-\frac{3}{4}\pi\mathrm{i})$, but it is otherwise arbitrary.

We find from this that $R_+(q)$ is finite as $q\to 0$; in fact, since

$$\int_0^{\infty}\frac{\ln_+(q/q_n)\,\mathrm{d}q}{q^2-q_n^2} = \frac{1}{q_n}\int_0^{\infty}\frac{\ln_+ t}{t^2-1}\mathrm{d}t = \frac{1}{q_n}\frac{\pi^2}{4}$$

(Gradshteyn & Ryzhik 1980, p. 532), we have

$$R_+(q) \sim \mathrm{e}^{-\frac{3}{4}\pi\mathrm{i}}\prod_{n=1}^{3}(q_n)^{\frac{1}{2}}\mathrm{e}^{\frac{1}{4}\pi\mathrm{i}} = 1, \tag{7.24}$$

and the next term can also be calculated and provides

$$R_+(q) \sim 1-\frac{2\mathrm{i}}{\sqrt{3}}q \quad \text{as} \quad q\to 0.$$

We also need the value of $R_+(q)$ at the value $q = \mathrm{e}^{\frac{2}{3}\pi\mathrm{i}}$ corresponding to the sinuous instability mode of wavenumber β given in (7.15). For this we need the values of

$$I_n = \int_{\exp(\frac{2}{3}\pi\mathrm{i})}^{\infty}\frac{\ln_+(q/q_n)\,\mathrm{d}q}{q^2-q_n^2}.$$

Of these, I_3 is an integral along a ray, and we put $q = t\,\mathrm{e}^{\frac{2}{3}\pi\mathrm{i}}$ and get

$$I_3 = \mathrm{e}^{-\frac{2}{3}\pi\mathrm{i}}\int_1^{\infty}\frac{\ln_+ t}{t^2-1}\mathrm{d}t;$$

the integral has half the value of one quoted before (7.24), so that

$$I_3 = \mathrm{e}^{-\frac{2}{3}\pi\mathrm{i}}\tfrac{1}{8}\pi^2.$$

For I_1 we deform the path from the ray through $e^{\frac{2}{3}\pi i}$ onto one round the unit circle to 1, then from 1 to $+\infty$. This gives

$$I_1 = -\frac{i}{2}\int_0^{\frac{2}{3}\pi} \frac{\theta \, d\theta}{\sin\theta} + \tfrac{1}{8}\pi^2.$$

For I_2, deform the path onto a segment of the unit circle from $e^{\frac{2}{3}\pi i}$ to $e^{\frac{1}{3}\pi i}$ and then a ray from $e^{\frac{1}{3}\pi i}$ to ∞. This gives

$$I_1 = -\frac{i}{2} e^{-\frac{1}{3}\pi i} \int_{\frac{1}{3}\pi}^{\frac{2}{3}\pi} \frac{(\theta - \frac{1}{3}\pi)\, d\theta}{\sin(\theta - \frac{1}{3}\pi)} + \tfrac{1}{8}\pi^2 e^{-\frac{1}{3}i\pi}.$$

Taking the appropriate linear combination of I_1, I_2 and I_3, and performing elementary manipulations, the integrals involving $\theta/\sin\theta$ cancel (they can in fact be evaluated in terms of Clausen's function Cl_2) and the final result is

$$R_+(e^{\frac{2}{3}\pi i}) = \surd 6\, e^{\frac{1}{6}\pi i}. \tag{7.25}$$

Finally, in order to check the edge behaviour, we need the asymptotics of $R_+(q)$ as $q \to \infty$. We readily find, directly from (7.23),

$$R_+(q) \sim e^{-\frac{3}{4}\pi i} q^{\frac{3}{2}} \left(1 + \frac{2i}{\surd 3 q} + O\left(\frac{1}{q^2}\right)\right). \tag{7.26}$$

It can then be checked that the solution obtained in §3 has the usual inverse square-root velocity and pressure singularity that one expects at a leading edge, while, when the Kutta condition is imposed at the duct exit edges, the solution of §6 has finite velocities and pressures, the shear layers leaving the duct lips with zero gradient at all times.

We end this section by setting down the results which are needed for simplification of the dispersion relation:

$$\alpha \sim \frac{\omega}{U_0}(-1 + iS^{\frac{1}{2}}), \quad \beta = -\gamma_\beta \sim \frac{\omega}{U_0} S^{-\frac{1}{3}}(-\tfrac{1}{2} + i\tfrac{1}{2}\surd 3), \tag{7.27 a, b}$$

$$H'(\beta) \sim 3bS^{-\frac{2}{3}} e^{-\frac{2}{3}\pi i}, \quad H_+(\beta) \sim -\surd 6\, e^{\frac{1}{6}\pi i}, \quad H_+(\alpha) \sim -1/(2S), \tag{7.27 c–e}$$

$$J_+(0) \sim b^{-\frac{1}{2}}, \quad K_+(i\epsilon) \sim \epsilon^{\frac{1}{2}} e^{\frac{1}{4}\pi i}, \quad K_+(\beta) \sim (6b)^{-\frac{1}{2}} S^{\frac{1}{3}} e^{\frac{5}{24}\pi i}, \tag{7.27 f–h}$$

and we assume in the result for $K_+(i\epsilon)$ that $\epsilon \ll |\beta|$, i.e. that the artificial cutoff length ϵ^{-1} greatly exceeds the largest relevant lengthscale $|\beta|^{-1}$ in the duct exit problem. These results in fact lead to a precise identification of ϵ. In the dispersion relation ϵ enters through the first term of (6.1), while it was proved in §5 that the correct result following from a uniformly accurate expression for the upstream feedback field is obtained by writing ζ for ϵ and carrying out $\int_0^\infty d\zeta$ with $G(\zeta)$ given by (5.16). Therefore ϵ is defined by

$$\frac{G}{K_+(i\epsilon)} = \int_0^\infty \frac{G(\zeta)\, d\zeta}{K_+(i\zeta)}$$

or

$$\frac{G}{\epsilon^{\frac{1}{2}} e^{\frac{1}{4}\pi i}} = -\frac{B}{\pi \alpha h} \frac{J_+(0) M_+(0)}{H_+(\alpha)},$$

where the right-hand side is estimated for $h \to \infty$ by applying Watson's lemma to the integral, and the left-hand side uses (7.27 g). When (7.27) are used again, together with (4.7) for G, we find

$$\epsilon = \frac{\pi}{4h}. \tag{7.28}$$

All the required conditions are satisfied by this choice of ϵ, and its use is fully equivalent to use of the uniformly valid forcing field (5.15)–(5.16) which, however, does not make clear the essential nature of that field near the duct exit – an oscillatory transverse streaming – in the way clearly revealed by the simpler (4.6).

8. The frequencies of the operating stages

When the asymptotic formulae (7.27) and (7.28) are used in the dispersion relation (6.1) it is found, on reduction, that

$$2\pi(h/b)\,S\exp\{-\tfrac{1}{2}\surd 3\,(h/b)\,S^{\frac{2}{3}}+\tfrac{5}{4}\pi\mathrm{i}-\tfrac{1}{2}\mathrm{i}(h/b)\,S^{\frac{2}{3}}\} = 1, \tag{8.1}$$

a relation of precisely the form postulated by Powell (1961). Imagine a disturbance released from the duct exit to comply with the Kutta condition there. It grows exponentially in space and its phase varies linearly with x as it propagates downstream, and its amplification and phase change over distance x are represented by an 'effectiveness' factor corresponding to the terms in $S^{\frac{2}{3}}$ in curly brackets of (8.1). The disturbance does not, however, immediately take the form of a freely propagating sinuous instability; there is a virtual origin for this instability which was, in effect, calculated in the duct exit problem in §5, and contributes to the $\frac{5}{4}\pi$ phase in (8.1). This virtual origin may also be referred to as corresponding to an 'end-correction', as in the classical problem of wave reflection from an open-ended pipe (see, e.g., Noble 1958, p. 138). Next, the disturbance interacts with the splitter plate, changing its wavenumber from β to α as analysed in §3 and generating, with a certain effectiveness factor, an upstream feedback field (§4), again with a virtual origin which contributes to $\frac{5}{4}\pi$ in (8.1). Apart from this virtual-origin effect, the upstream feedback involves no spatial phase change, as it involves a purely irrotational motion with algebraic decay in space, leading to the algebraic factor $2\pi h/b$ in (8.1). The feedback field then perturbs the jet at the duct exit with a certain effectiveness, and this, through the Kutta condition, provokes the release of a subsequent disturbance an integral number of periods later in the phase-locked feedback cycle. Evidently the product of the 'effectiveness factors' round the feedback loop must come to unity, and this is precisely what (8.1) expresses. Our contribution has been to provide analytical expressions, from low-frequency linear theory, for the Powell effectiveness factors and for the virtual-origin effects.

The phase content of (8.1) will be adopted, as explained in §1, and gives

$$\omega b/U_0 = (b/h)^{\frac{3}{2}}[4\pi(N-\tfrac{3}{8})]^{\frac{3}{2}} \tag{8.2}$$

for $N = 1, 2, 3, \ldots$, showing that for given values of U_0, b, h, ω may have any one of a countable series of values which give different *stages* of operation. In a given stage, ω varies linearly with U_0, increases with b as $b^{\frac{1}{2}}$, and decreases as $h^{-\frac{3}{2}}$ as h increases. These are the general properties sought from the model and typical of edge-tone behaviour in a variety of geometrically different configurations. The functional form of (8.2) is also in agreement with a range of experiments, as can be seen from figure 4, which will be discussed in a moment. Another way of presenting (8.2) involves the wavelength $\lambda_0 = 2\pi/|\mathrm{Re}\,\beta|$ of the sinuous instability mode; using (7.27 *b*) and (8.2), we have

$$h/\lambda_0 = N-\tfrac{3}{8}. \tag{8.3}$$

An expression of this kind, $h/\lambda_0 = N+\epsilon$ for some constant numerical ϵ, has been widely sought and used in the literature on shear-layer feedback cycles, and $\epsilon = \frac{1}{4}$ is commonly used on the basis of the classic experiments of Brown (1937 *a*, *b*). It says

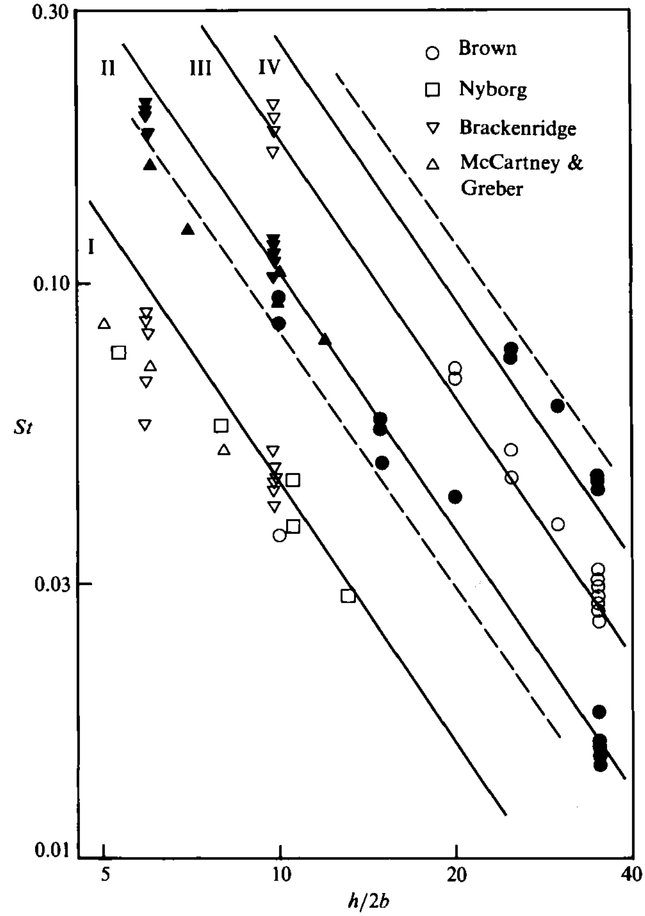

FIGURE 4. Variation of Strouhal number $St = S/\pi$ with stand-off distance $h/2b$ (taken from Holger *et al.* 1977). Symbols indicate measured data taken by experimenters named, and referenced here. ——, Predictions of theory of Holger *et al.* (1977) with some degree of parameter adjustment; ----, predictions of present theory (equation (8.2)) for the lowest two modes, no adjustment.

that the stand-off distance contains an integral number of hydrodynamic wavelengths plus an end correction to account for local effects near the jet exit and near the splitter-plate edge. However, it is not obvious that the end corrections should appear simply as one constant for all N, and it is far from obvious that the constant, if it exists, is universal. Rather, one would expect it to depend rather critically on the detailed geometry of the upstream and downstream bodies, so that our prediction $\epsilon = -\frac{3}{8}$ would be expected to differ from what might be found in a typical experiment (say, with wedge, and a slit in a large plane wall). There is, indeed, considerable scatter in the experimental literature on this point, and our model should emphasize the fact that only the form of (8.3) is significant, not the numerical value of ϵ.

Consider now figure 4 in more detail. This figure, taken from Holger *et al.* (1977), compares experimental data taken by Brown (1937*a*, *b*), Nyborg (1954), Brackenridge (1960) and McCartney & Greber (1973) with predictions of a model worked out by Holger *et al.* This model represents the jet as an alternating vortex street, and deals in some detail with the interaction of the street with the same splitter plate as in this paper. It does not, however, seriously analyse the motion near the jet exit, using instead a simple phase-reversal argument to account for the presence of the duct walls and to identify the phase at which the next vortex is added to the street. This procedure does not incorporate any end correction for the nozzle exit. Further, there are several adjustable parameters in the model of Holger *et al.* and this restricts the extent to which theirs is a rational deductive model. Nonetheless, as figure 4 shows, that model does lead to rather good agreement with experiment if the parameters are suitably chosen, even though it may be less appropriate for flows such as that of figure 3, when there is no evidence of any concentrations of vorticity (other than in *continuous* shear layers) upstream of the splitter plate.

Now figure 4 also shows the predictions of the present theory for $N = 1, 2$, and we see that while our theory and that of Holger *et al.* (1977) agree very closely in the functional dependence, they differ significantly in an overall factor. To be precise, the theory of Holger *et al.* gives, in the notation of this paper,

$$\omega b/U_0 = 8.22(b/h)^{\frac{3}{2}}(N+\epsilon_N)^{\frac{3}{2}} \tag{8.4}$$

with slight changes in the ϵ_N from one stage to another: $\epsilon_1 = 0.40$, $\epsilon_2 = 0.35$, $\epsilon_3 = 0.50$. The coefficient 8.22 in (8.4) is much smaller than $(4\pi)^{\frac{3}{2}} \approx 44.55$. Accordingly, the main discrepancy between (8.2) and (8.4) is associated with a phase contribution $S^{\frac{2}{3}}h/2b$ in (8.1) which is much larger than that in the Holger *et al.* model – and indeed much larger than that measured (albeit indirectly). This discrepancy is entirely associated with the free amplification and propagation of the sinuous β-mode, the contributions of the end corrections being much smaller, and it brings to light an aspect of hydrodynamic stability theory not, apparently, previously noted.

The discrepancy is equivalent to one between the phase speed c of the sinuous mode and the propagation speed V of the vortex street of Holger *et al.* In the limit $S \to 0$, (7.27*b*) gives

$$c/U_0 \approx 2S^{\frac{1}{3}}, \tag{8.5}$$

while (1.20) of Holger *et al.* gives

$$V/U_0 = 0.945(S/\pi)^{\frac{1}{3}} = 0.645S^{\frac{1}{3}}. \tag{8.6}$$

There is no necessary connection between c and V: indeed, Holger *et al.* say that any correspondence 'may be simply fortuitous since there is no reason why a linear theory should correctly predict the properties of a stable configuration in the nonlinear range'. Since those words were written, however, considerable evidence has accumulated, as mentioned in §1, to support the idea that the propagation speed and transverse structure of nonlinear modes on jet flows can indeed be quite well predicted by linear theory – provided the correct flow profile is used. We have modelled the profile in a very special way, and have also used low-frequency asymptotics to determine β and c, and both simplifications are possible sources of error.

First, consider different velocity profiles in the limit $S \to 0$. In the parallel-flow idealization, all profiles $U(y) = U_1 F(y/\delta)$ must conserve not only the momentum flux in the jet,

$$M = \int_{-\infty}^{+\infty} \rho U^2 \, \mathrm{d}y$$

but also the volume flux

$$Q = \int_{-\infty}^{+\infty} U \, \mathrm{d}y$$

and if Q and M are given, the values of U_1 and δ can be determined, for a given profile F, in terms of the U_0, b for the top-hat jet. Then the results of Drazin & Howard

(1966) for long-wavelength temporal instability can be used, and inverted for spatial instability at low frequency, to predict β as a function of ω as $\omega \to 0$. It is found that the leading-order behaviour is independent of F, the instability depending only on the values of M and Q. Higher-order terms (in ω) are similar, but have numerical coefficients which differ depending on the profile F. Profile sensitivity is probably not very important, therefore.

The inversion process indicates, however, that while the long-wavelength temporal instability results have quite a wide range of applicability, their inverses for spatial instability are useful only at very low frequencies. Consider, for example, the sinuous mode relation (3.19) for temporal instability; then β is real and negative, and for $\beta b \to 0$,

$$\omega b/U_0 \sim (\beta b)^2 + (\beta b)^3 + \ldots + \mathrm{i}(-\beta b)^{\frac{3}{2}}(1+\beta b + \ldots) \tag{8.7}$$

on the unstable branch. The series for $\mathrm{Re}\,\omega$ and $\mathrm{Im}\,\omega$ are essentially geometric, in powers of βb, and the leading terms of each are good for $\beta b \ll 1$. Inversion gives, however, for spatial instability,

$$\beta b \sim \mathrm{e}^{2\pi \mathrm{i}/3}(\omega b/U_0)^{\frac{2}{3}} - \tfrac{2}{3}(\omega b/U_0) + \ldots \tag{8.8}$$

and the series, of which (7.27b) is the first term, proceeds very slowly, with comparable real and imaginary parts, in powers of $(\omega b/U_0)^{\frac{1}{3}}$. The first term dominates only at very low frequencies, and this is why (8.5) leads to such high phase speeds c (higher than U_0) at quite small values of S. A better prediction is obtained by taking $\mathrm{Re}\,\beta$ from the first two terms in (8.8), and gives

$$\frac{c}{U_0} \approx \frac{2S^{\frac{1}{3}}}{1+\frac{4}{3}S^{\frac{1}{3}}}, \tag{8.9}$$

the effect of the denominator being to roughly halve the value of c in (8.5) at $S = 0.3$ – though higher terms ought probably then also to be included.

We conclude from this that low-frequency spatial stability asymptotics are valid only at *very* low frequencies, and that the principal reason for the discrepancy between (8.3) and experiment is associated with the use in (7.27b) of simply the leading-order approximation for β. Much better agreement could presumably be reached on the basis of (8.9), or an expression including further terms in $S^{\frac{1}{3}}$; all such expressions would lead to the same behaviour, namely preservation of essentially the form of (8.2), but with $(4\pi)^{\frac{3}{2}}$ replaced by a smaller coefficient which is actually a slowly varying function of frequency. This in turn would imply that an expression like (8.2) could be fitted to the calculated results, with a smaller constant coefficient than $(4\pi)^{\frac{3}{2}}$ but with a number ϵ_N replacing the constant $(-\frac{3}{8})$ and varying slowly from one stage to another. Such a representation was indeed arrived at by Holger *et al.* (1977) (see (8.4) above) on the basis of a model with a number of *ad hoc* assumptions. We do not pursue closer agreement with experiment here; the idea of our model is to provide analytical insight in simple expressions from clearly defined and rational problems.

9. Displacement thickness waves on the splitter plate

We consider now the possible significance of displacement thickness fluctuations in the boundary layers over the splitter plate. Howe (1981 a, b, c and later papers) has written extensively on this topic, and shown that in some configurations these fluctuations – with an amplitude determined by the imposition of a leading-edge

Kutta condition – can have a strong effect on the flow through a slot or aperture. We shall find here a similarly significant effect on the amplitude of the upstream feedback forcing field studied in §4, and will indeed find total cancellation of that field in a particular limit which is easily interpreted. When that total cancellation does not occur, however – and it will not in fact occur – we find that the displacement thickness fluctuations do not change the phase of the feedback field. There is thus no change to the frequencies of the operating stages (on linear theory) which were discussed in §8. There is, on the other hand, a very definite change to the structure of the acoustic field, as will be discussed in a separate paper.

The idea is that we add to the antisymmetric (in y) field of §3 an eigenfunction for the splitter plate which is associated with antisymmetric fluctuations of the displacement thickness of the boundary layers on the two sides of the plate. Such an eigenfunction has the same type of leading-edge singularity as that studied in §3, and a leading-edge Kutta condition (Goldstein 1981; Howe 1981*a*, *b*, *c*; Crighton 1985) can be used to determine the amplitude V of displacement thickness fluctuations. We need to assume that the displacement thickness fluctuations (DTF) are of fine scale on the scale of the jet width $2b$ (and hence on the hydrodynamic scale U_0/ω of the large-scale instability waves), otherwise strong coupling would exist between the boundary-layer motion and that of the jet shear layers. This coupling would preclude modelling of the DTF via a condition

$$\partial\phi/\partial y = -\partial\psi/\partial y = V\mathrm{e}^{\mathrm{i}\kappa X} \tag{9.1}$$

on $y = 0, 0 < X < \infty$ (equation (3.16)) with a wavenumber κ determined by the mechanics of the boundary-layer flow in isolation from the jet flow.

Suppose then that (9.1) is accepted, as in the numerous papers by Howe, with $\kappa b \gg 1$. Then the eigensolution for the splitter plate is obtained by solving

$$\nabla^2\phi = 0$$

in $-\infty < X < +\infty, y > 0$, with

$$\phi = 0 \quad \text{on} \quad y = 0, \quad X < 0, \tag{9.2}$$

equation (9.1) on the splitter plate $y = 0, X > 0$, and with $\psi(X, y) \equiv -\phi(X, -y)$. The jet boundaries $y = \pm b$ have effectively been taken to infinity under the assumption $\kappa b \gg 1$. Standard Wiener–Hopf analysis then leads to

$$\phi(X, y) = -\frac{\mathrm{i}V}{2\pi\gamma_-(-\kappa)}\int_{-\infty}^{+\infty}\frac{\exp(-\mathrm{i}kx - \gamma y)\,\mathrm{d}k}{(k+\kappa)\,\gamma_+(k)}, \tag{9.3}$$

where $\gamma(k) = k$ if $\mathrm{Re}\,k > 0$, $-k$ if $\mathrm{Re}\,k < 0$, and $\gamma_\pm(k)$ are the Wiener–Hopf factors of $\gamma(k)$ as identified in (7.17). This solution can be shown to have an $X^{-\frac{1}{2}}$ singularity in pressure and velocity which cancels that of the solution obtained in §3 if V is appropriately chosen. With this choice of V, the upstream feedback field associated with DTF, given generally by

$$\phi = \frac{\mathrm{e}^{-\frac{1}{4}\pi\mathrm{i}}V}{2\pi^{\frac{1}{2}}(\kappa h)^{\frac{3}{2}}}y = G^{(1)}y, \tag{9.4}$$

is found to have coefficient

$$G^{(1)} = -(\omega/\kappa U_0)\,G, \tag{9.5}$$

where

$$G = -\frac{\mathrm{i}BJ_+(0)}{2\pi^{\frac{1}{2}}\alpha h^{\frac{3}{2}}\mathrm{e}^{\frac{1}{4}\pi\mathrm{i}}H_+(\alpha)}$$

is the coefficient associated with the upstream feedback field in the absence of DTF (see (4.7)). In obtaining (9.5), use has been made of the various estimates at the close of §7.

The total feedback field is proportional to $(1-\omega/\kappa U_0)$ and vanishes if $\kappa = \omega/U_0$. This is easily understood (though not actually permitted in the model, which requires $\kappa U_0/\omega \gg 1$) when one notes that then the value of $\partial\phi/\partial y$ on $y = 0, X < 0$ and the contribution corresponding to $\Phi'_-(k,0)$ from (3.11) sum to give (to leading order for $\omega b/U_0) \ll 1$) *zero normal velocity* on the upstream extension of the splitter plate. No mode conversion from an incident β-mode in $X < 0$ to an emergent α-mode in $X > 0$ then takes place, and there is no upstream feedback field. There is no suggestion that such a cancellation actually takes place, however, and the hypothetical case $\kappa = \omega/U_0$ is noted merely as a point to check.

Generally, κ will exceed ω/U_0. Howe (1981*b*) considers the case of a boundary layer with linearly increasing velocity from 0 to U_0 over a range δ in y, for which Rayleigh obtained the dispersion relation for temporally growing waves as

$$\omega = U_0\kappa - \frac{U_0}{2\delta}(1-e^{-2\delta\kappa}),$$

and for the condition imposed at $y = \delta$ to be transferred as in (9.1) to $y = 0$ we require $\kappa\delta \ll 1$. Then

$$\kappa \approx \frac{\omega}{U_0}\left(\frac{U_0}{\omega\delta}\right)^{\frac{1}{2}} \gg \frac{\omega}{U_0}, \tag{9.6}$$

and even if the $\gg$ sign is replaced by $>$, it is now clear that the imposition of a leading-edge Kutta condition makes absolutely no change to the phase relation which determines the frequencies of the operating stages. A more significant change occurs in the acoustic field, but discussion of that field is deferred to a separate paper.

10. Discussion

The main conclusions of this paper have already been set out, in §§1, 8 and 9, and will not be reiterated. Brief comments are in order, however, on one or two aspects of the work.

First, the notion of causality was raised in §3. A causal solution to a time-harmonic steady-state problem is analytic in frequency in the upper half-plane $\operatorname{Im}\omega > 0$. Now in Wiener–Hopf problems such as those of §§3 and 5, solutions are found as integrals along the real axis of wavenumber space using certain analyticity requirements in k-space in relation to upper and lower half-planes $\operatorname{Im} k \gtrless 0$ (strictly speaking a strip of overlap is needed, but that is irrelevant to the present point). When ω varies in $\operatorname{Im}\omega > 0$, however, poles in k-space do not necessarily remain on the same side of the real k-axis, and indeed those representing spatial instability waves cross from one half-plane to the other. Analyticity in ω can then only be preserved by deformation of the integration path in k-space to prevent this, the upper and lower halves of k-space then lying above and below this deformed contour, respectively. This was first explained in relation to the interaction between a vortex sheet and a rigid plate, with external acoustic forcing, by Crighton & Leppington (1974) and Morgan (1974). The deformation procedure implies, for example, that in the factorization of $(\tau+1)^2+S$ in (7.18), both factors should be included in the 'minus' function and the lower half-plane regarded as including the point $\tau = -1+\mathrm{i}S^{\frac{1}{2}}$. A spatially bounded solution is then sought with this interpretation of 'upper' and 'lower' and found as an integral along the deformed path. This integral may in turn be written as one along the real k-axis plus a residue term from the pole (at $\tau = -1+iS^{\frac{1}{3}}$ in the example quoted) which is exponentially growing in space. Such a procedure automatically generates the appropriate spatial instabilities, and could have been used here. In §3 there would have been no 'forcing' and the primary terms in (3.5) would not have been initially separated out, but would have been produced as residues in the way just mentioned (for the varicose wave). In §5 the transverse forcing would have been retained but the allocation of factors to different split functions would have led to two possibilities for the Wiener–Hopf entire function. One would have given zero residue and a field bounded at $x = +\infty$ – the field of §5 in fact. The other would have ensured satisfaction of the Kutta condition, and then the residue contribution would have given a residue field corresponding precisely to the eigensolution (5.18) with the correct choice of A_1, namely that of (6.1). A similar discussion is given in relation to a leading-edge problem by Goldstein (1981). We emphasize, therefore, that the solutions obtained here comply with the causality principle, but the exponential growth in x has been extracted at the outset, in (3.5) and (5.18), rather than produced by contour deformations accounting for causality.

Examination of causality issues fails, however, to resolve a somewhat unsatisfactory aspect of the leading-edge splitter-plate problem studied in §3. We noted there that the solution, expressed in the form (3.17) appropriate to $X < 0$, has a pole contribution at $k = \alpha$ corresponding to the varicose mode, one at $k = \beta$ for the sinuous mode (giving (3.23)), and a branch-line contribution studied in §4. Now it becomes apparent, from the low-frequency approximation (7.9) to the sinuous mode dispersion function $M(k)$, that there is in (3.17) a further pole contribution which will appear for $X < 0$ (and for some range of $Y = y-b$ certainly including $Y = 0$), namely that from the pole at $q = e^{\frac{1}{3}\pi i}$, or

$$k = -\beta^* = (\omega/U_0)\, S^{-\frac{1}{3}}\{\tfrac{1}{2}+i\tfrac{1}{2}\sqrt{3}\} \tag{10.1}$$

(cf. (7.15)). The mode to which this gives rise is, in a sense, perfectly acceptable for $X < 0$; it is identical to (3.23) with β replaced by $-\beta^*$, and thus decays as $X \rightarrow -\infty$ at the same rate as the 'sinuous mode' (3.23). It has $\operatorname{Re} k$ equal and opposite to that of the sinuous mode, however, so that as X increases from large negative values the mode given by (10.1) grows in space in precisely the same way as the genuine sinuous instability wave, but 'propagates' towards $X = -\infty$ rather than $X = +\infty$. Such a curious 'backward-propagating spatial instability' could not appear in $X > 0$, of course. Indeed, Hardisty (1974) has proved that the rectangular jet at low Mach number (as here) has precisely two spatial instability modes at each ω, one varicose and one sinuous. The corresponding wavenumbers $k = \alpha$ and $k = \beta$ cross the real axis from below to their final positions (7.14) and (7.15), respectively, as ω moves from a position high up in $\operatorname{Im}\omega > 0$ down to the real value of ultimate interest. Such modes propagate to $X = +\infty$ and will in general appear downstream of any excitation or inhomogeneity; the β-mode does not occur in the splitter-plate problem because it cannot satisfy the condition on $y = 0$.

The field corresponding to (10.1) thus causes no difficulties at all for $X > 0$, where it never appears. To interpret its appearance for $X < 0$ one simply has to assert that while $k = \beta$ gives rise to an 'incident' sinuous mode (3.23), $k = -\beta^*$ gives rise to a 'reflected' sinuous mode. The reflected mode propagates towards $X = -\infty$, the incident away from $X = -\infty$; both decrease towards $X = -\infty$ at the same rate. Both have to be distinguished by their physical structure from the feedback field, represented by the branch-line integral, which is much less small as $X \rightarrow -\infty$. Making that distinction on physical grounds, rather than mathematical, is a familiar point; see the discussion in Crighton (1981, p. 282) of Goldstein (1981), and observe also that Goldstein takes no account of the reflected β mode in his analysis of a leading-edge splitter-plate problem with external acoustic (or gust) forcing. How the distinction can justifiably be made mathematically is a point needing further investigation – as also are the physical features associated with nonlinear shear-layer dynamics and the acoustic field of the jet edge-tone device. These topics will be taken up in future work, but a remark is in order on nonlinearity of the shear-layer motions. Until recently, nonlinear effects in free-shear layers appeared to be destabilizing (Huerre 1980), so that a suitably normalized (real) amplitude a would evolve in space according to an equation of the form

$$\mathrm{d}a/\mathrm{d}x = a+\mu a^3, \quad \mu > 0. \tag{10.2}$$

Such an equation could not lead to the kind of finite-amplitude periodic limit cycle behaviour that is often thought to underlie edge-tone operation (see, for example, Blake & Powell 1986; Karamcheti *et al.* 1969; Nyborg 1954). Huerre (1987) and Churilov & Shukhman (1987) have, however, now discovered a further contribution to the Landau constant μ in (10.2) which is large, and of the opposite sign, implying that nonlinear effects are strongly stabilizing. Thus the correct amplitude equation reads

$$\mathrm{d}a/\mathrm{d}x = a(a_*^2-a^2), \tag{10.3}$$

and a asymptotes to a_* in a limit cycle. The extension of these ideas to a jet flow, rather than a single free shear layer, and their combination with the linear calculations presented here for the interactions with upstream and downstream boundaries, should provide a nonlinear theory to predict the amplitude and frequency of the edge-tone stages.

This work was supported by the Office of Naval Research under Grants N00014-81-0010 and N00014-86-G-0066, monitored by Dr R. L. Sternberg, and Mr M. Blizard, Code 425.

REFERENCES

Blake, W. K. & Powell, A. 1986 The development of contemporary views of flow-tone generation. In *Recent Advances in Aeroacoustics* (ed. A. Krothapalli & C. A. Smith), pp. 247–235. Springer.

Brackenridge, J. B. 1960 *J. Acoust. Soc. Am.* **32**, 1237–1242.

Brown, G. B. 1937*a* *Proc. Phys. Soc. Lond.* **49**, 439–507.

Brown, G. B. 1937*b* *Proc. Phys. Soc. Lond.* **49**, 508–521.

Churilov, S. M. & Shukhman, I. G. 1987 *Proc. R. Soc. Lond.* A **409**, 351–367.

Cohen, J. & Wygnanski, I. 1987*a* *J. Fluid Mech.* **176**, 191–219.

Cohen, J. & Wygnanski, I. 1987*b* *J. Fluid Mech.* **176**, 221–235.

Crighton, D. G. 1972 *J. Fluid Mech.* **56**, 683–694.

Crighton, D. G. 1981 *J. Fluid Mech.* **106**, 261–298.

Crighton, D. G. 1985 *Ann. Rev. Fluid Mech.* **17**, 411–445.

Crighton, D. G. & Leppington, F. G. 1974 *J. Fluid Mech.* **64**, 393–414.

Curle, N. 1953 *Proc. R. Soc. Lond.* A **216**, 412–424.

Drazin, P. G. & Howard, L. N. 1966 *Adv. Appl. Mech.* **9**, 1–89.

Durbin, P. A. 1984 *J. Fluid Mech.* **145**, 275–285.

Fletcher, N. H. 1979 *Ann. Rev. Fluid Mech.* **11**, 123–146.

GASTER, M., KIT, E. & WYGNANSKI, I. J. 1985 *J. Fluid Mech.* **150**, 23–39.

GOLDSTEIN, M. E. 1981 *J. Fluid Mech.* **104**, 217–246.

GRADSHTEYN, I. S. & RYZHIK, I. M. 1980 *Table of Integrals, Series and Products*. Academic.

HARDISTY, M. 1974 The effect of sound on vortex sheets. Ph.D. thesis, University of Dundee.

HOLGER, D. K., WILSON, T. A. & BEAVERS, G. S. 1977 *J. Acoust. Soc. Am.* **62**, 1116–1128.

HOURIGAN, K., WELSH, M. C., THOMPSON, M. C. & STOKES, A. N. 1990 *J. Fluids Struct.* **4**, 345–370.

HOWE, M. S. 1981*a* *Proc. R. Soc. Lond.* A **374**, 543–568.

HOWE, M. S. 1981*b* *J. Sound Vib.* **75**, 239–250.

HOWE, M. S. 1981*c* *J. Sound Vib.* **74**, 311–320.

HUERRE, P. 1980 *Phil. Trans. R. Soc. Lond.* A **293**, 643–675.

HUERRE, P. 1987 *Proc. R. Soc. Lond.* A **409**, 369–381.

KARAMCHETI, K., BAUER, A. B., SHIELDS, W. L., STEGEN, G. R. & WOOLLEY, J. P. 1969 Some features of an edge-tone flow field. *NASA* SP-207, pp. 275–304.

KRANZER, H. C. & RADLOW, J. 1962 *J. Math. Anal. Applics.* **4**, 240–256.

KRANZER, H. C. & RADLOW, J. 1965 *J. Math. Mech.* **14**, 41–59.

KROTHAPALLI, A. & HORNE, C. 1984 Recent observations on the structure of an edge-tone flow field. *AIAA* 84-2296.

MCCARTNEY, M. S. & GREBER, I. 1973 *Case Western Reserve University FTAS TR*-73-87.

MÖHRING, W. F. 1978 *J. Fluid Mech.* **85**, 685–691.

MORGAN, J. D. 1974 *Q.J. Mech. Appl. Maths* **27**, 465–487.

NOBLE, B. 1958 *Methods Based on the Wiener–Hopf Technique*. Pergamon.

NYBORG, W. L. 1954 *J. Acoust. Soc. Am.* **26**, 174–182.

ORSZAG, S. A. & CROW, S. C. 1979 *Stud. Appl. Maths* **49**, 167–181.

POWELL, A. 1961 *J. Acoust. Soc. Am.* **33**, 395–409.

ROCKWELL, D. & NAUDASCHER, E. 1979 *Ann. Rev. Fluid Mech.* **11**, 67–94.

STAUBLI, T. & ROCKWELL, D. 1987 *J. Fluid Mech.* **176**, 135–167.

STONEMAN, S. A. T., HOURIGAN, K., STOKES, A. N. & WELCH, M. C. 1988 *J. Fluid Mech.* **192**, 455–484.

STRANGE, P. J. R. & CRIGHTON, D. G. 1983 *J. Fluid Mech.* **134**, 231–245.